

Application of a new phosphorus-free palladium heterogeneous nanocatalyst supported on modified MWCNT the highly selective and efficient cleavage of propargyl, allyl, and benzyl phenol ethers under mild conditions

Hashem Sharghi¹ · Abbas Khoshnood¹ · Reza Khalifeh² ·
Mohammad Mehdi Doroodmand¹

Received: 17 April 2014 / Accepted: 21 March 2015 / Published online: 17 April 2015
© Springer International Publishing Switzerland 2015

Abstract A stable and efficient phosphorus-free, low Pd-loading heterogeneous nanocatalyst comprising palladium and a multi-walled carbon nanotube was prepared and characterized by various techniques such as SEM, TEM, AFM, FT-IR, and Raman spectrometry, N₂ adsorption isotherm and thermogravimetric analysis. This catalyst was used for the deprotection of phenol ethers. The catalyst selectivity for deprotection of between propargyl, allyl, and benzyl, as a protecting group, was studied. Also, the presence of different functional groups was studied to establish the scope and limitations of this method. The catalytic activity of recycled catalyst was evaluated. The results indicated that the catalyst is heterogeneous, stable, and very active under the established conditions, and it could be reused up to five times without any significant leaching. In addition, according to ICP analysis, low leaves of leaching of palladium from the catalyst was observed, which indicates that anthraquinone has an excellent ability to coordinate with palladium.

Keywords Heterogeneous nanocatalyst · Deprotection · Multi-walled carbon nanotube · Anthraquinone · Phosphorus free · Palladium catalyst

Introduction

The protection and deprotection of heterofunctional groups are common practices in multistep organic transformations

✉ Hashem Sharghi
shashem@susc.ac.ir

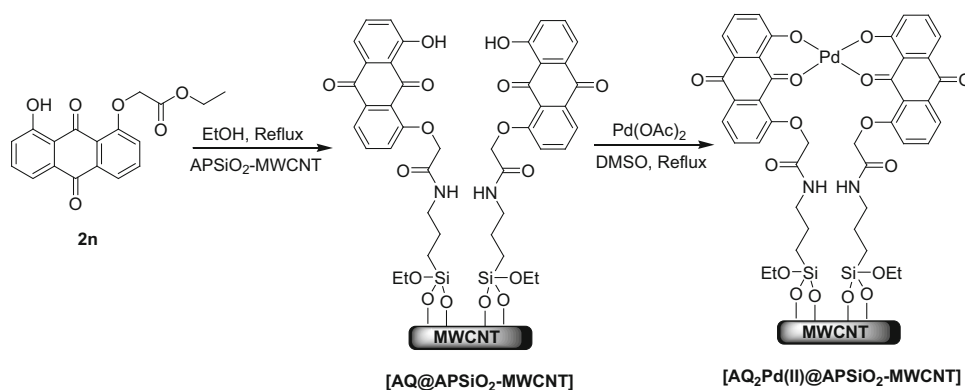
¹ Department of Chemistry, Shiraz University, 71454 Shiraz, Iran

² Department of Chemistry, Shiraz University of Technology, 71555-313 Shiraz, Iran

and synthesis of complex molecules, especially in the synthesis of natural products and polyfunctional molecules [1–3]. In addition, the ability or inability for the compatibility and selective deprotection of a specific protecting group in the presence of another under mild conditions is often a key to the success or failure of a synthetic route [4]. The phenolic hydroxyl group exists in diverse kinds of chemical compounds as represented by the large number of natural products in plant and animal life. Therefore, numerous protecting groups have been developed for phenol protection [5]. Allyl, propargyl, and benzyl moieties are the most commonly used for the protection of phenolic hydroxyl groups [6]. A suitable protecting group is the allyl unit, due to its stability under acidic as well as basic and reductive conditions [1]. The wide applicability of the allyl group is indicated by several publications [7], likely because of the straight forward synthesis of allyl ethers from a phenol with an allyl halide in the presence of a base. In the case of propargyl and benzyl groups, the former is less preferred as a protecting group compared to the allyl group because of the lack of a convenient and selective deprotecting protocol, while the latter is the most commonly used “persistent” protecting group in carbohydrate, peptide, and alkaloid chemistry [1, 8].

Among them, the propargyl group is more attractive due to the presence of two orthogonal π -bonds, which can help in its facile cleavage in the presence of transition metal complexes [9]. The conversion of ethers to phenols can be carried out in presence of various reagents and catalysts; however, the success of the transformation largely depends on the proper choice of deprotecting reagents and catalysts which are compatible with other functional groups in the multifunctional compounds. Available methods include NBS [10], DDQ [11], SmCl₃ [12], TiCl₃ [13], NaBH₄/I₂ [14], CeCl₃ · 7H₂O/ NaI [15], BBr₃ [16], low-

Scheme 1 Synthesis of new heterogeneous catalyst [AQ₂Pd(II)@APSiO₂-MWCNT]



valent titanium [17], and nickel-catalyzed electroreductions [18].

A wide variety of palladium catalysts have efficiently promoted some deprotection reactions and usually require phosphorus ligands [19,20]. Phosphorus ligands are widely used to stabilize the palladium catalysts, but they are unpleasant to work with due to their cost, toxicity, and sensitivity to air/moisture. Thus, Pd–phosphine complexes are not favored for use in large scale industrial applications [21]. A number of Pd complexes as catalyst with non-phosphine ligands, having different donor functionalities, have been synthesized and their catalytic activities have been studied [22]. In the synthesis of drugs, the possibility of having palladium-containing impurities in the final product can lead to unfavorable toxicities. This is especially a significant problem for *in vivo* studies becoming a significant challenge to the medicinal chemist [23]. Although there are methods reduce and bring Pd to acceptable levels [23], ultimately the best solution is not use palladium catalysts if possible. From practical, economic, and environmental standpoints, it is desirable to use a solid catalyst without hazardous additives such as phosphine as a green alternative to the conventional homogeneous processes. The appropriate pore-size distributions of carbon nanotubes (CNTs) could favor maximum metallic dispersion [24,25]. CNTs are suitable to be used as hybrid catalysts because they are composed of a metal complex anchored on a solid support, their morphology and steady structural properties. Also, hybrid catalysts do not have many disadvantages of homogeneous and heterogeneous catalysts [26]. In continuation of our previous studies to utilize a heterogeneous catalyst for the synthesis of organic compounds [27–32], in this article we wish to report a new, phosphorus-free, and reusable nanocatalyst system based on palladium anthraquinone attached to MWCNT. This heterogeneous catalyst system displays an excellent catalytic operation for deprotection reactions of phenol ether derivatives. Moreover, the heterogeneous catalysts can be repeatedly used for this transformation and subsequently recovered after the reaction. Also the palladium leaching is very negligible.

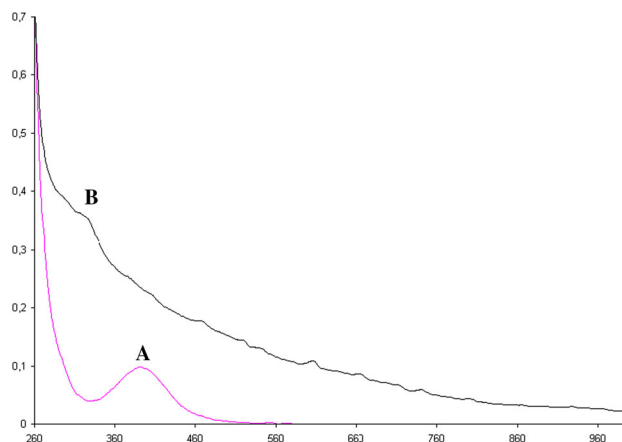


Fig. 1 Monitoring the supporting process of Pd(OAc)₂ by UV–Vis, **a** before and **b** after being supported on the [AQ₂Pd(II)@APSiO₂-MWCNT]

Results and discussion

The typical strategy to obtain the aforementioned heterogeneous palladium catalyst is to modify MWCNT with a ligand. The metalloanthraquinone catalysts immobilized on a modified carbon nanotube were readily prepared in a two-step procedure. Before the direct use of the multi-walled carbon nanotubes (MWCNT), its surface was first modified by inserting hydroxy groups (OH) by means of gas phase oxidation under air. The modified MWCNT was refluxed with triethoxysilylpropylamine in absolute ethanol for 5 h. An aminopropyl silica gel MWCNT (APSiO₂-MWCNT) was refluxed with hydroxy-8-ethylacetate anthraquinone in absolute ethanol for 48 h. In the next step, the AQ@APSiO₂-MWCNT was allowed to reflux with an excess amount of palladium acetate in DMSO for 12 h (Scheme 1).

The reaction process was followed by UV–Vis spectroscopy (Fig. 1). As it can be observed, the UV–Vis spectra of Pd(OAc)₂ revealed a signal at 400 nm referring to the presence of Pd(II). The usual Pd(II) signal at 400 nm disappeared due to the formation of AQ₂Pd(II)@APSiO₂-MWCNT.

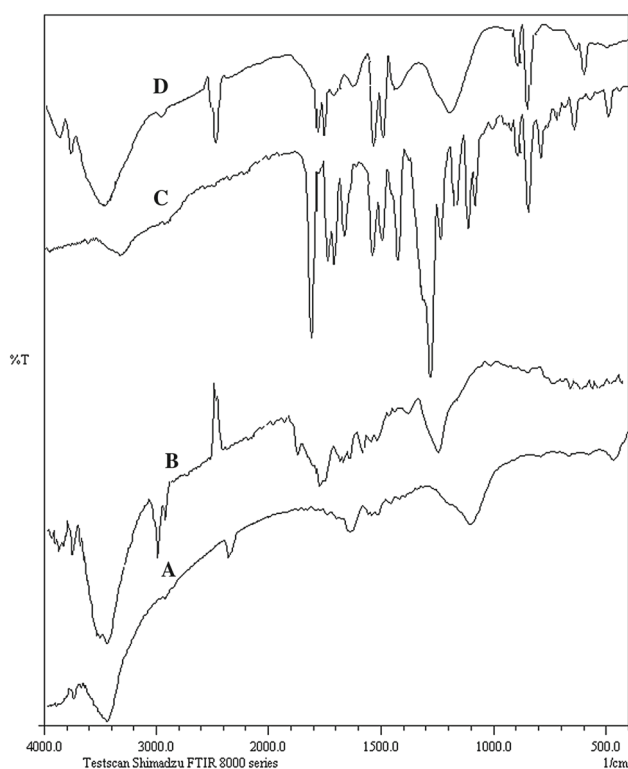


Fig. 2 FT-IR spectrum of **a** activated MWCNT, **B** APSiO₂-MWCNT, **c** AQ, and **d** AQ@APSiO₂-MWCNT

The resulting supported complexes were separated, washed with water, dried and their anchoring on MWCNT was examined by FT-IR spectroscopy. Figure 2a–d shows the FT-IR spectra of activated MWCNT, APSiO₂-MWCNT, anthraquinone ligand (**2n**), and AQ@APSiO₂-MWCNT, respectively. According to Fig. 2a, the sharp signal at 3218 cm⁻¹ corresponds to the OH functional groups. Significant enhancement in the intensity of the signal at 3223 cm⁻¹ reveals the immobilization of SiO₂ on the activated MWCNT (Fig. 2b). Based on Fig. 2c, the strong signals at 1731, 1719, and 1706 cm⁻¹ correspond to the carbonyl groups of ester and AQ, respectively. Major reduction in the intensity of the absorption bands related to the bending of N–H bond at ~1600 cm⁻¹ indicate the chemical immobilization of AQ on the APSiO₂-MWCNT (Fig. 2d). Furthermore, comparison between the spectra of AQ and that of the one supported on APSiO₂-MWCNT shows a chemical immobilization of AQ on APSiO₂-MWCNT. As observed in Fig. 1d, the lack of an absorption band at 1731 cm⁻¹ shows the amide formation during the immobilization of AQ on APSiO₂-MWCNT.

The synthesized AQ₂Pd(II)@APSiO₂-MWCNT was also characterized using Raman spectrometry as shown in Fig. 3. Modification of AQ₂Pd(II)@APSiO₂-MWCNT is evaluated according to the signal area of the D-band (~1350 cm⁻¹). Based on the Raman spectrum (Fig. 3), the defect of AQ₂Pd(II)@APSiO₂-MWCNT was evaluated to 3.15, which

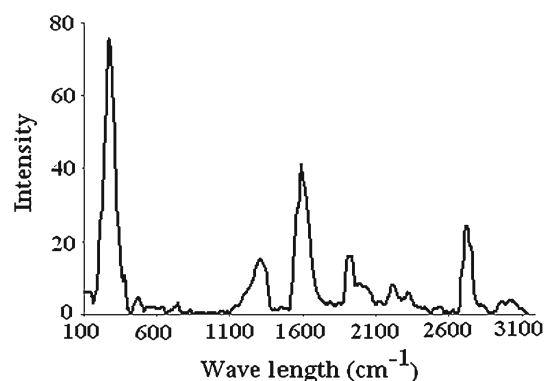


Fig. 3 Raman spectrum of AQ₂Pd(II)@APSiO₂-MWCNT

remarkably is higher than that obtained for activated MWCNT (4.32). An average diameter to ~20 nm was also evaluated for the MWCNT based on the radial breathing mode (RBM) of the Raman spectrum at 216 cm⁻¹ (Fig. 3).

The morphology of Pd nanoparticles immobilized on AQ@APSiO₂-MWCNT is shown according to the AFM image (Fig. 4a). Pd nanoparticles with normal size distribution (Fig. 4a) were synthesized using the proposed procedure. Based on the AFM image, the histogram shown in Fig. 4b shows the average size of Pd nanoparticles (~40 nm).

Figure 5a shows the SEM image of AQ₂Pd(II)@APSiO₂-MWCNT, synthesized by the described method. Also, Figure 5b–d shows the TEM images of (b) activated MWCNT, (c) APSiO₂-MWCNT, and (d) AQ@APSiO₂-MWCNT. Based on the SEM and TEM images, the average diameter of MWCNT matrix was evaluated to ~30 nm. The presence of the same correlation between the average diameters (~30 nm) pointed to stability of MWCNT before and after immobilization of AQ by the recommended procedure. However, separation in the MWCNT matrix was observed when AQ is chemically bonded to APSiO₂-MWCNT.

According to the smoothed XRD picture displayed in Fig. 6, the signal positioned at around 15° is related to the silica gel support. Also, the signal positioned at 2θ is equal to 47° correlating to the different palladium phase (Pd(200)) [33].

To estimate the palladium content, the supported catalyst was treated with 5.0 M HCl and HNO₃ for analyzed by ICP. The palladium content was determined to be 2.07 % w/w, which is close to the expected value of 2.11 % w/w.

Based on Fig. 7, partial enchantment in the weight percentage of the thermogram at temperatures to ~320°C is attributed to the decomposition of the complex and formation of palladium oxides. In addition, significant reduction in the weight percentage of the thermogram at temperature to ~540°C reveals the oxidation of MWCNT and formation of carbon oxides. The weight percentage of generated palladium

Fig. 4 a AFM image and b histogram of Pd nanoparticles immobilized on AQ@APSiO₂-MWCNT

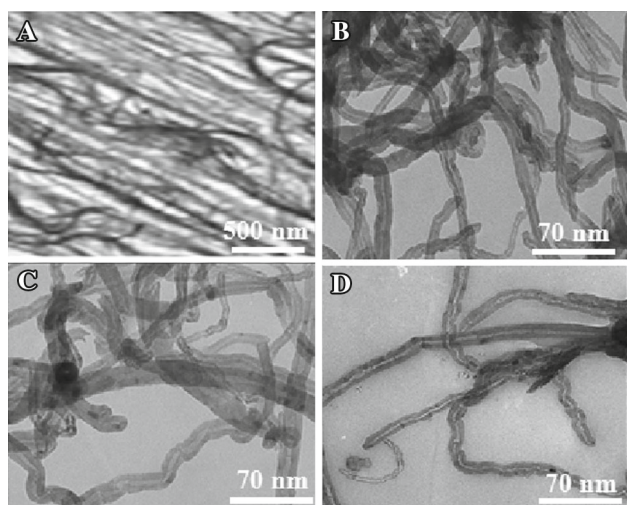
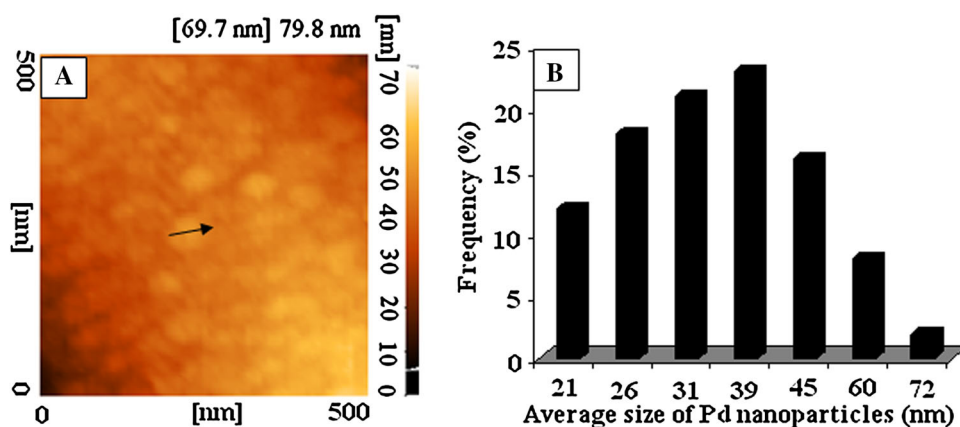


Fig. 5 Electron microscopic images including a SEM of AQ₂Pd(II)@APSiO₂-MWCNT, b TEM of activated MWCNT, c TEM of APSiO₂-MWCNT, and d TEM of AQ@APSiO₂-MWCNT

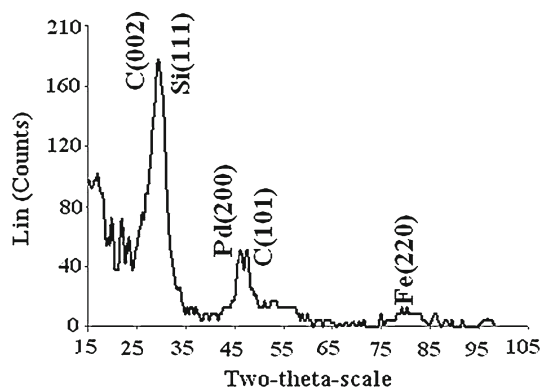


Fig. 6 XRD pattern of AQ₂Pd(II)@APSiO₂-MWCNT

oxide can be determined using the end part of the thermogram. Based on the amount of oxygen needed for oxidation of Pd and formation of the palladium oxide, the quantity of Pd immobilized on the AQ@APSiO₂-MWCNT is estimated at ~2.11 % (w/w).

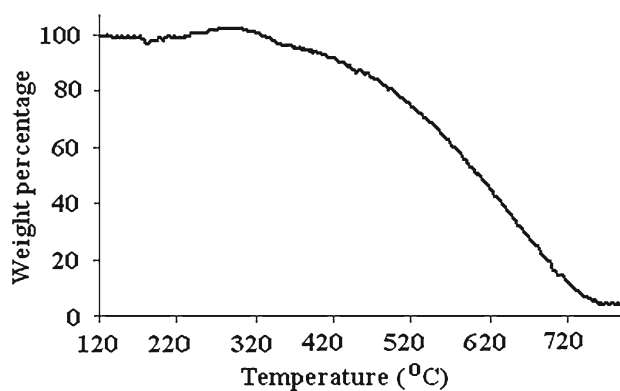


Fig. 7 Thermogram of AQ₂Pd(II)@APSiO₂-MWCNT

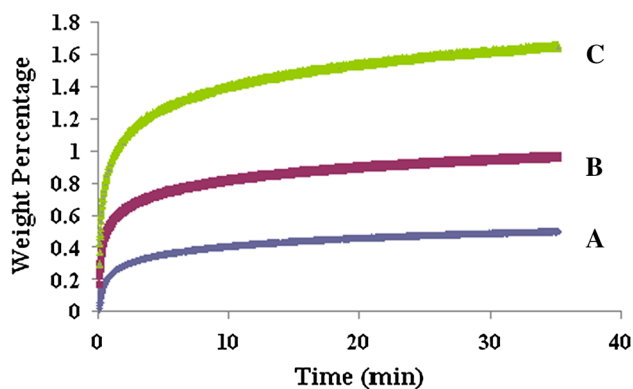
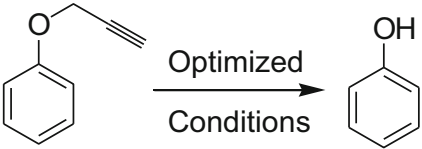


Fig. 8 Nitrogen-adsorption isotherm of a Activated MWCNT, b APSiO₂-MWCNT, and c AQ₂Pd(II)@APSiO₂-MWCNT

The nitrogen adsorption of the palladium anthraquinone complex on MWCNT validated that the palladium anthraquinone complex was well coated on the MWCNT. This technique was achieved via flowing a trace amount of nitrogen gas through the sample and following the changes in the weight percentage of palladium supported on MWCNT using the TG analysis as shown in Fig. 8. According to nitrogen-adsorption isotherms, significant change from 231 to 519 m² g⁻¹ was observed in the active sur-

Table 1 Deprotection reaction of propargyl-protected phenol under different reaction conditions


C#CCOc1ccccc1
 $\xrightarrow[\text{Conditions}]{\text{Optimized}}$
Oc1ccccc1

Entry	Catalyst (mol%)	Temperature (°C)	Solvent	Base	Time (min)	Yield (%)
1	–	25 and 100	–	Cs ₂ CO ₃	60	0
2	Pd(OAc) ₂ (5)	100	–	Cs ₂ CO ₃	60	8
3	[AQ ₂ Co(II)@APSiO ₂ -MWCNT] (5)	100	–	Cs ₂ CO ₃	60	26
4	[AQ ₂ Fe(II)@APSiO ₂ -MWCNT] (5)	100	–	Cs ₂ CO ₃	60	47
5	[AQ ₂ Ni(II)@APSiO ₂ -MWCNT] (5)	100	–	Cs ₂ CO ₃	60	41
6	[AQ ₂ Cu(II)@APSiO ₂ -MWCNT] (5)	100	–	Cs ₂ CO ₃	60	68
7	[AQ ₂ Pd(II)@APSiO ₂ -MWCNT] (5)	100	–	Cs ₂ CO ₃	60	94
8	[AQ ₂ Pd(II)@APSiO ₂ -MWCNT] (5)	25	–	Cs ₂ CO ₃	60	0
9	[AQ ₂ Pd(II)@APSiO ₂ -MWCNT] (2)	100	–	Cs ₂ CO ₃	60	70
10	[AQ ₂ Pd(II)@APSiO ₂ -MWCNT] (10)	100	–	Cs ₂ CO ₃	60	98
11	[AQ ₂ Pd(II)@APSiO ₂ -MWCNT] (5)	Reflux	NMP	Cs ₂ CO ₃	60	30
12	[AQ ₂ Pd(II)@APSiO ₂ -MWCNT] (5)	Reflux	EtOH	Cs ₂ CO ₃	60	42
13	[AQ ₂ Pd(II)@APSiO ₂ -MWCNT] (5)	100	DMSO	Cs ₂ CO ₃	60	78
14	[AQ ₂ Pd(II)@APSiO ₂ -MWCNT] (5)	Reflux	CH ₃ CN	Cs ₂ CO ₃	60	36
15	[AQ ₂ Pd(II)@APSiO ₂ -MWCNT] (5)	Reflux	H ₂ O	Cs ₂ CO ₃	60	12
16	[AQ ₂ Pd(II)@APSiO ₂ -MWCNT] (5)	100	–	–	60	0
17	[AQ ₂ Pd(II)@APSiO ₂ -MWCNT] (5)	100	–	K ₂ CO ₃	60	74
18	[AQ ₂ Pd(II)@APSiO ₂ -MWCNT] (5)	100	–	NaOH	60	16
19	[AQ ₂ Pd(II)@APSiO ₂ -MWCNT] (5)	100	–	DABCO	60	19
20	[AQ ₂ Pd(II)@APSiO ₂ -MWCNT] (5)	100	–	<i>t</i> -BuOK	60	11
21	[AQ ₂ Pd(II)@APSiO ₂ -MWCNT] (5)	100	–	Et ₃ N	60	35
22	[AQ ₂ Pd(II)@APSiO ₂ -MWCNT] (5)	100	–	<i>i</i> -pr ₃ N	60	30
23	[AQ ₂ Pd(II)@APSiO ₂ -MWCNT] (5)	100	–	Pyridine	60	14

face area of MWCNT substrate during immobilization of AQ₂Pd(II)@APSiO₂. Significant enhancement in the active surface area of AQ-immobilized MWCNT revealed good immobilization of AQ by the introduced method.

To clarify the requirement of reagents and conditions for deprotection of phenol ethers, the reactions of propargyl-protected phenol as a model were carried out and the results are summarized in Table 1.

Based on our literature survey, we applied a transition metal as catalyst, tetrabutylammonium bromide (TBAB) as a scavenger for protecting groups, and a base for optimization of the reaction condition. In the absence of catalyst, prop-2-ynyloxy-benzene is stable at room temperature and 100 °C for more than 60 minutes (Table 1, entry 1). When the reaction was performed in the presence of Pd(OAc)₂ (5 mol%) as a catalyst, TBAB as propargyl scavenger, cesium carbonate as base under solvent-free condition at 100 °C, the reaction yield was slightly increased (Table 1, entry 2). This result encouraged us to further investigate this reaction. In the

next step, the catalytic activities of various heterogeneous metalloanthraquinone complexes attached to multi-walled carbon nanotube [AQ₂M(II)@APSiO₂-MWCNT], which were synthesized similar to palladium anthraquinone as non-phosphine catalyst, were also examined in the model reaction (Table 1, entries 3–7). Among several stable metalloanthraquinone carbon nanotubes screened, we found palladium anthraquinone to be quite efficient: the reaction completed at 100 °C during 60 min in the presence of 5 mol% of this catalyst under solvent free condition, while the reaction proceeded relatively slowly in the presence of other metalloanthraquinone under the same conditions (Table 1, entries 3–6). The reactions were usually carried out at 100 °C in the presence of 5 mol% catalyst for 60 min under solvent-free conditions. Lowering the temperature was found to be inefficient based on the yields of products (Table 1, entry 8). The optimal amount of catalyst was found to be 5.0 mol%. A decrease in the amount of catalyst resulted in a significant reduction of the yield while an increased amount of cata-

lyst has a negligible effect on the efficiency of the reaction (Table 1, entries 7, 9, 10). After optimization of both reaction temperature and catalyst performance, we subsequently turned our attention toward a screening of solvent effects (Table 1, entries 11–15). The reaction does not proceed in quantitative conversions in any solvent, with DMSO giving only a slightly better yield of unprotected phenol. Solvent-free condition was found to be the most effective media in term of fast reaction rate, high yield, selectivity, and environmental acceptability. It has been shown that the base plays an important role in facilitating the reaction. At this point, the influence of the base was investigated. A variety of different organic and inorganic bases were tested. On the basis of these results, only cesium carbonate gave a high conversion rate, although K_2CO_3 produced the product in a 74 % yield (Table 1, entries 17–23).

Having found the optimized conditions in hand, we subsequently turned our attention toward the exploration of the scope and the limitation of our process (Table 2).

In another reaction, propargyl 2-naphthyl ether was cleaved to 2-naphthol within 60 min at 100 °C in high yield (Table 2, entry 2). Anthraquinone, xanthone, and coumarin containing a variety of functional groups were readily alkylated to generate a series of substituted anthraquinone, xanthone, and coumarin propargyl ethers derivatives. Anthraquinone and xanthone propargyl ether react in the presence of a catalyst under our optimized conditions to yield the desired products in high yield (Table 2, entries 3–6). It is significant that α , β -unsaturated lactones, such as coumarins, were not affected by this catalyst as exemplified by the smooth deprotection of 7,8-dipropargyloxycoumarin to 7,8-dihydroxycoumarin (Table 2, entry 7). According to the selectivity of our methodology, when using substrates containing easily reducible groups, such as the reaction of *p*-nitro propargyl ether with this catalyst was carried out to obtain *p*-nitro phenol in 87 % yield (Table 2, entry 8).

Dehalogenation was observed in some other methods, when a substrate contained halogen groups [34]. Thus, we used our methodology with these compounds and no dehalogenated product was detected (Table 2, entries 9, 10). The reaction of propargyl ethers containing an isolated C=C bond led to the formation of the corresponding compounds with the C=C bond intact (Table 2, entries 11, 12). The reactions of anthraquinone propargyl ethers with ester moieties were achieved in 96 % yield (Table 2, entries 13, 14).

The reaction performance using allyl ethers instead of propargyl ethers was also studied. Accordingly, the allyl ethers of phenol, anthraquinone, and coumarin were converted to their corresponding alcohols in high yields under optimized conditions at appropriate time (Table 2, entries 15–19). Furthermore, some allyl ethers containing various functional groups were synthesized and their deprotection

was investigated under optimized conditions and the corresponding products were obtained in high yields (Table 2, entries 20–25).

During our attempts to explore the ability of catalyst, we observed that when using benzyl ethers as substrates they were cleaved under the optimized reaction conditions. For example, benzyloxybenzene was converted to its corresponding phenol using a mixture of catalyst (5 mol%), TBAB, and cesium carbonate (Table 2, entry 26). To investigate further the scope and versatility of the optimized system for debenzilation, several different protected derivatives were synthesized and examined (Table 2, entries 27–33).

Selective cleavage of one ether in the presence of another is often needed in the synthesis of more complex compounds. Therefore, the regioselective cleavage between allyl and propargyl ethers has been investigated. Normally, palladium reagents can deprotect both allyl and propargyl groups without any discrimination. Interestingly, when the anthraquinone ether containing both allyl and propargyl groups was treated with our catalyst, the anthraquinone containing allyl group was isolated in excellent yield. This selectivity is very remarkable and is not normally observed with other reagents used for the deprotection of ethers (Table 2, entries 34). It should be noted that, according to the proposed mechanism, the complex formed between palladium and the π -electrons of the propargyl group is more stable than the complex of palladium with the π -electrons of the allyl and benzyl groups. This is because of a higher electron density of π bond in the propargyl group vs. the allyl and benzyl groups; therefore, the catalyst shows better selectivity toward propargyl groups over the allyl and benzyl groups. With these results, we used an anthraquinone derivative protected with propargyl and benzyl groups as a substrate and demonstrated its selective transformation. Treating this compound under our optimized condition removed the propargyl moiety to yield corresponding compound quantitatively, whereas benzyl ether moiety did not react at all (Table 2, entry 35). Additionally, propargylic ester along with the ether was not cleaved under the reaction conditions, and treatment of this compound with our catalyst caused depropargylation from the propargyl ether in high yield. Thus, this method is suitable for the deprotection of propargylic ethers of *O*-propargyl-protected acids without interfering with the protection of the acid group (Table 2, entry 36).

Alkoxy groups such as methoxy, propargylic amide, and propargyl ether of alcohols, remained unaffected during the course of the reaction, even after increasing the reaction time to 350 min (Table 2, entry 37–40).

We carried out the model reaction on a 100-mmol scale in the presence of the heterogeneous catalyst in order to assess the feasibility of applying this method in a preparative scale. This reaction proceeded similar to the smaller scale (Table 3,

Table 2 Regioselective deprotection of various ethers using AQ₂Pd(II)@APSiO₂-MWCNT under solvent-free reaction conditions

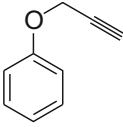
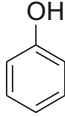
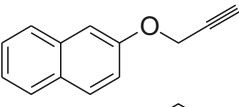
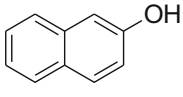
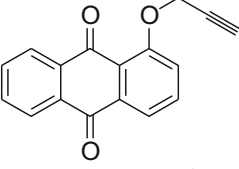
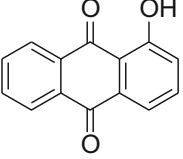
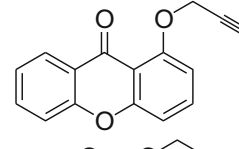
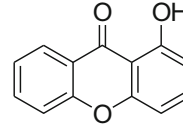
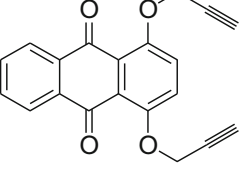
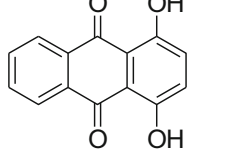
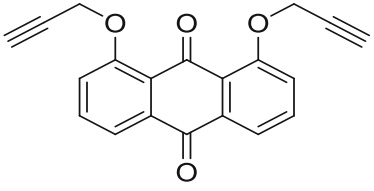
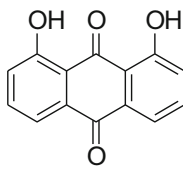
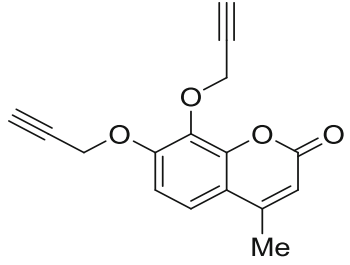
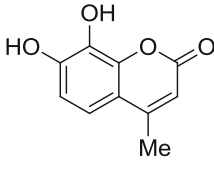
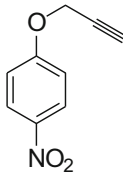
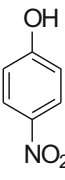
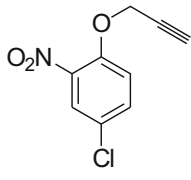
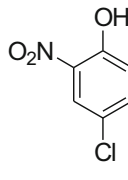
Entry	Catalyst (mol%)	Product	Time (min.)	Yield (%)	
1			2a	60	94
2			2b	60	95
3			2c	60	93
4			2d	45	90
5			2e	60	96
6			2f	60	96
7			2g	60	90
8			2h	45	87
9			2i	45	90

Table 2 continued

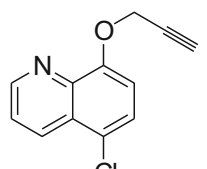
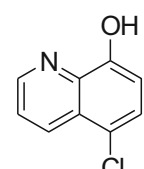
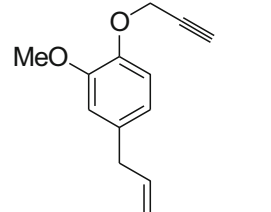
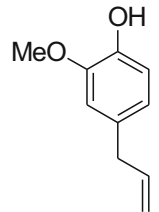
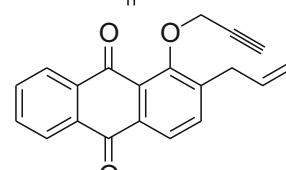
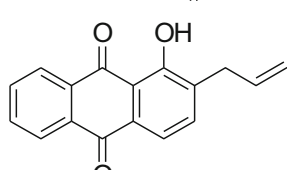
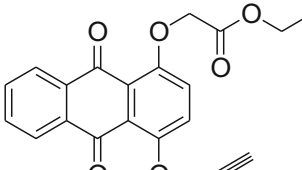
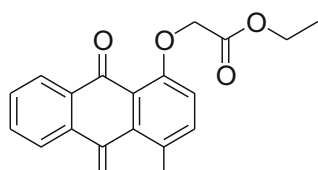
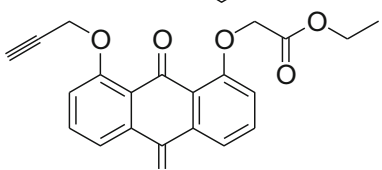
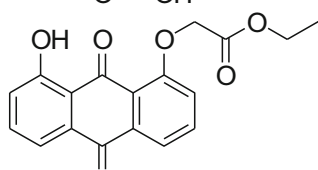
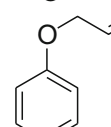
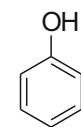
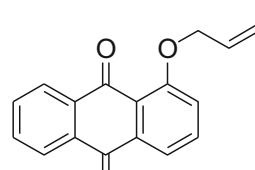
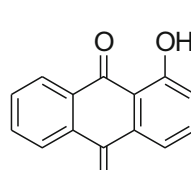
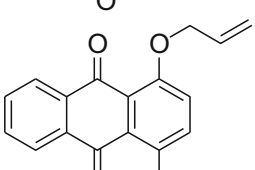
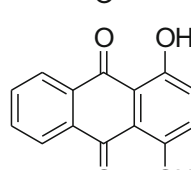
Entry	Catalyst (mol%)	Product	Time (min.)	Yield (%)	
10			2j	60	84
11			2k	90	97
12			2l	60	97
13			2m	45	96
14			2n	45	96
15			2a	60	91
16			2c	60	95
17			2e	60	95

Table 2 continued

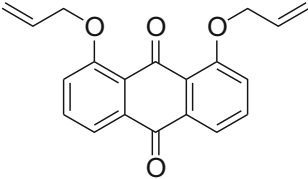
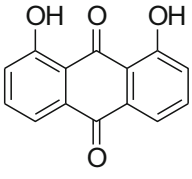
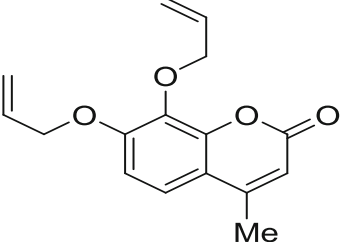
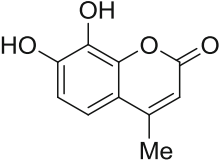
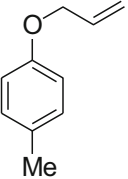
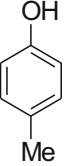
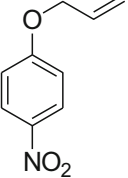
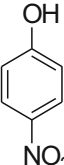
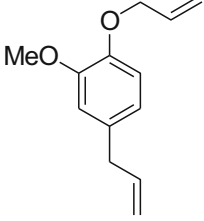
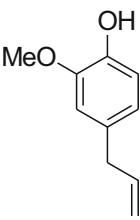
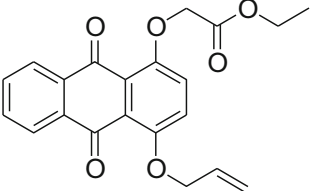
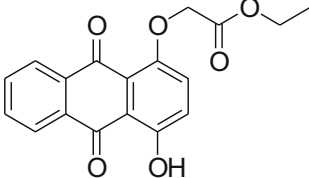
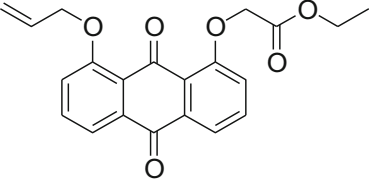
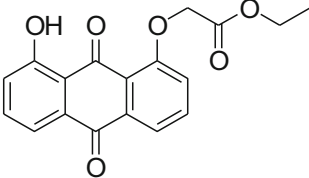
Entry	Catalyst (mol%)	Product	Time (min.)	Yield (%)	
18			2f	60	92
19			2g	60	90
20			2o	60	88
21			2h	45	91
22			2k	90	95
23			2m	45	94
24			2n	45	94

Table 2 continued

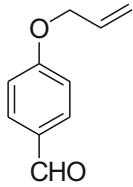
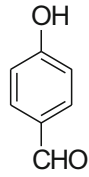
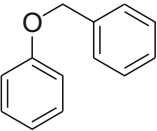
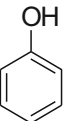
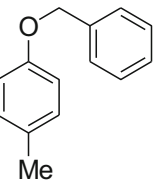
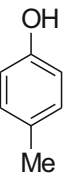
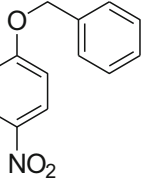
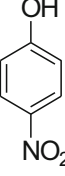
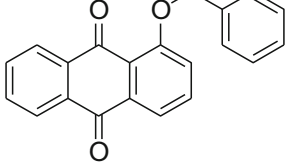
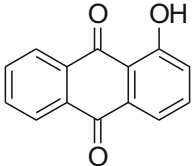
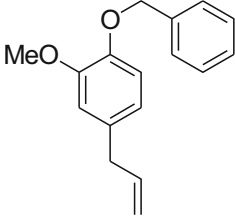
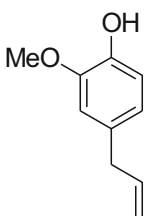
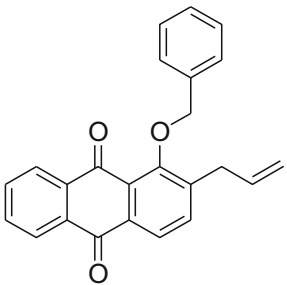
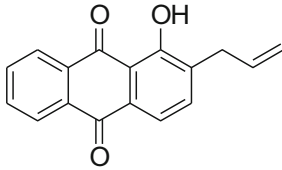
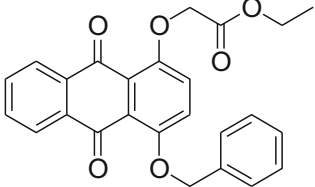
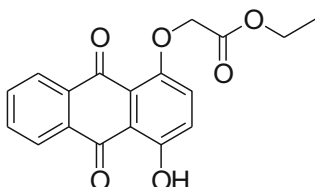
Entry	Catalyst (mol%)	Product	Time (min.)	Yield (%)	
25			2p	45	86
26			2a	60	93
27			2q	60	87
28			2h	40	96
29			2c	90	94
30			2k	90	96
31			2l	60	95
32			2m	60	94

Table 2 continued

Entry	Catalyst (mol%)	Product	Time (min.)	Yield (%)	
33			2n	45	95
34			2r	45	93
35			2s	45	96
36			2t	45	91
37			2e	350	0
38			2u	350	0
39			2v	350	0
40			2w	350	0

In the standard conditions, the reactions were carried out at 100°C in the absence of solvent containing AQ₂Pd(II)@APSiO₂-MWCNT (5 mol%), *n*-Bu₄N⁺Br⁻ (TBAB) and cesium carbonate as base for 60 min

Table 3 Recycling of the [AQ₂Pd(II)@APSiO₂-MWCNT] nanoparticle catalyst for the deprotection of prop-2-ynyloxy-benzene in 60 min

Run	Isolated yield (%)
1	98
2	96
3	96
4	93
5	92

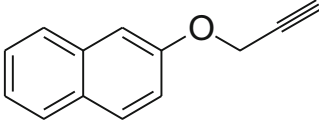
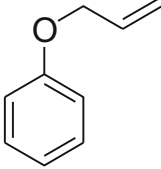
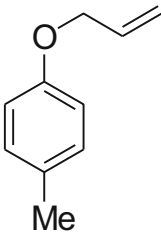
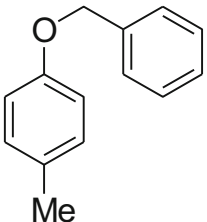
entry 1), and the desired product was isolated in 98 % yield after 1 h.

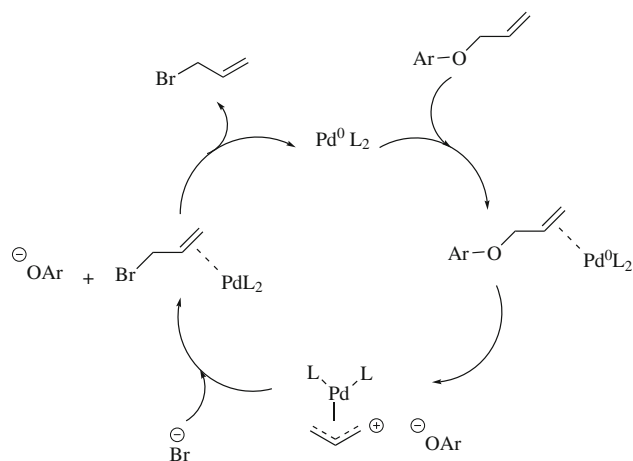
The recyclability of the heterogeneous catalyst was tested in the deprotection of prop-2-ynyloxy-benzene. The catalyst was recovered by simply filtration and after washing with appropriate solvent, it was used again directly without further purification up to five successive runs. The recovered heterogeneous catalyst was analyzed with ICP after five consecutive runs and 2.03 % (w/w) of Pd was discovered, which can be compared to the initial value of 2.07 % (w/w), showing of less than 0.04 % leaching during the reaction cycles.

A comparison of the catalytic efficiency of AQ₂Pd(II)@APSiO₂-MWCNT with selected previously known catalysts is collected in Table 4 to demonstrate that the present protocol is indeed superior to several of the other protocols. The other listed methodologies in this table suffer from limitations such as high temperatures, high catalyst cost (e.g., [CpRu(CH₃CN)₃]PF₆/L), prolonged reaction times (e.g., CeCl₃ · 7H₂O, NaI), complexity of ligand (e.g., Pd/L) or low yields.

While the detailed mechanism for the deprotection of propargyl ethers by palladium complex is unclear at this stage, a proposed mechanism of the palladium-catalyzed deallylation reaction is offered in Scheme 2. The palladium(0) nanoparticles were produced in situ from Pd(OAc)₂/TBAB/Cs₂CO₃ system [40]. After a prior coordination to the double bond, presumably the C–O bond cleavage proceeds via displacement of the Pd⁰ L₂ fragment with the leaving group [−]OAr leading to a π-allyl complex. This π-allyl complex then undergoes a nucleophilic attack by a bromide anion, thereby releasing the desired products with the

Table 4 Comparison of protocols for the deprotection of propargyl, allyl, and benzyl ethers

Entry	Ether	Condition	Catalyst	Time	Yields (%)	Ref.
1		ArSH, K ₂ CO ₃ , NMP, N ₂ , 210 °C	[AQ ₂ Pd(II)@APSiO ₂ -MWCNT]	15 min	72	[35]
		TBAB, Cs ₂ CO ₃ , solventless, 100 °C		1 h	95	–
2		MeOH, 30 °C	[CpRu(CH ₃ CN) ₃]PF ₆ /L	3 h	99	[36]
		1,3-Propanedithiol, CH ₃ NO ₂ , reflux	CeCl ₃ · 7H ₂ O, NaI	32 h	30	[37]
		Aniline, 30 °C	Pd/L	20 min	98	[19]
		TBAB, Cs ₂ CO ₃ , solventless, 100 °C	[AQ ₂ Pd(II)@APSiO ₂ -MWCNT]	1 h	91	–
3		MeOH, KOH, r.t	Pd/C	96 h	17	[38]
		THF, 70 °C	Pd(PPh) ₄ /L	24 h	100	[20]
		DMF, NaOAc, r.t	Electrogenerated Ni	18 h	76	[18]
		TBAB, Cs ₂ CO ₃ , solventless, 100 °C	[AQ ₂ Pd(II)@APSiO ₂ -MWCNT]	1 h	88	–
4		THF, DMEU, 185 °C, sealed tube	LDA	12 h	87	[39]
		TBAB, Cs ₂ CO ₃ , solventless, 100 °C	[AQ ₂ Pd(II)@APSiO ₂ -MWCNT]	1 h	87	–



Scheme 2 Proposed mechanism for the cleavage of allyl ethers

regeneration of Pd(0) species completing the catalytic cycle [41].

Conclusions

In this study, we have reported a reproducible and simple synthetic method for a recyclable phosphorus-free heterogeneous palladium nanocatalyst supported on modified MWCNT. We have analyzed the surface, the morphology, and total composition of new catalyst by IR, ICP, XRD, SEM, and AFM analyses. With this catalyst, a new and efficient deprotection reaction for the phenol ether has been developed. Furthermore, the selectivity between propargyl, allyl, and benzyl group as a protecting group was investigated. The scope of the deprotection reaction using our catalyst is completely wide; various propargyl, allyl, and benzyl ethers react readily at 100 °C in solventless reaction condition. Moreover, the catalyst can be recovered by simple filtration of the reaction solution and reused for at least five consecutive trials without becoming less in the activity.

Experimental section

Instrumentation, analyses, and starting material

General Chemical materials were either prepared in our laboratories or were purchased from Aldrich, Fluka, or Merck Companies. The purity determination of the substrates and reaction monitoring were accomplished by TLC on silica gel PolyGram SILG/UV254 plates or by a Shimadzu Gas Chromatograph (GC-10A) instrument. Mass spectra were determined on a Shimadzu GCMS-QP 1000 EX instruments at 70 or 20 eV. An atomic force microscopy (AFM, DME-SPM, version 2.0.0.9) was used for AFM images. Spectroscopic methods including X-ray diffraction (XRD,

D8, Advance, Bruker, axs) and FT-IR spectrometry (Shimadzu FT-IR 8300 spectrophotometer) were obtained for characterization of the heterogeneous catalyst. Elemental analyses were performed with a Thermo Finnigan CHNS-O analyzer, 1112 series. NMR spectra were recorded on a Bruker Avance DPX-250 (^1H NMR 250 MHz and ^{13}C NMR 62.9 MHz) in pure deuterated solvents with tetramethylsilane (TMS) as an internal standard (s, singlet; d, doublet; t, triplet; q, quartet; dd, doublet of doublet; m, multiplet). Scanning electron micrographs were obtained by SEM instrumentation (SEM, XL-30 FEG SEM, Philips, at 20 KV). The TG analysis of the samples was performed with a lab-made TG analyzer instrument. Briefly, it consisted of a T-shaped glass tube with 20-cm height, whose base was put vertically on a gravimeter (Mettler Company, model 3640). A quartz tube with 1.5-cm i.d. and 20-cm long was put on the other two sides of the T-shaped tubes. The quartz tube was gone inside a furnace (15 cm length) without direct connection. Another movable quartz tube with diameter of 0.5 cm was used as sample cell, which was put inside the other quartz tube. Before any analysis, the accuracy as well as the precision of the designed TG analyzer were evaluated using reference materials such as amorphous carbon. After calibration of the system, it was adopted for evaluation of the morphology as well as the weight percentage of the synthesized nanocatalyst.

Metal contents were obtained by ICP analysis (Varian, vista-pro). UV/Vis. spectra were obtained with an Ultrospec 3000 UV/Visible spectrometer. Melting points were determined in open capillary tubes in a Buchi-535 circulating oil melting point apparatus.

Compounds **1c**, **1e**, **1am**, **2m** [29]; **1a**, **1h** [31], and **1f** [32] have been reported previously, and all data were consistent with those published in the literature.

(8-Hydroxy-9,10-dioxo-9,10-dihydro-anthracen-1-yloxy)-acetic acid ethyl ester (**2n**)

Ethyl 2-bromoacetate (0.5 mmol, 0.11 mL) was added to a solution of 1,8-dihydroxyanthraquinone (1.0 mmol, 0.24 g) and *t*-BuOK (0.5 mmol, 0.05 g) in DMF (25 mL). After the completion of the reaction at room temperature for 24 h, the reaction mixture was poured onto cold water. The product was isolated with simple filtration as shiny yellow crystals with 91 % yield.

mp = 198 °C. R_f = 0.64 (50 % *n*-Hexane: 50 % EtOAc). IR (KBr) ν = 3425.3, 2993.3, 1735.8, 1674.1, 1635.5, 1573.8, 1450.4, 1280.6, 1226.6, 1033.8, 779.2, 740.6 cm^{-1} . ^1H NMR (250 MHz, CDCl_3) δ = 1.23 (t, J = 7.1 Hz, 3H), 4.22 (q, J = 7.1 Hz, 2H), 4.80 (s, 2H), 7.13–7.21 (m, 2H), 7.49–7.68 (m, 3H), 7.91 (d, J = 7.6 Hz, 1H), 12.80 (s, 1H) ppm. ^{13}C NMR (62.9 MHz, CDCl_3) δ = 14.14, 61.73, 66.47, 106.00, 117.00, 118.87, 119.95, 121.37, 124.76, 132.54, 135.50,

135.97, 158.88, 162.44, 167.97, 182.50, 188.50, 193.50 ppm. MS: m/z (%) = 328 (3.2, $M^+ + 2$), 327 (10.5, $M^+ + 1$), 326 (24.8, M^+), 280 (14.9), 253 (100.0), 224 (87.0), 196 (16.8), 168 (16.8), 139 (57.3), 111 (13.1), 97 (29.0), 83 (32.7), 69 (38.9), 57 (69.7). Anal. Calcd for $C_{18}H_{14}O_6$ (326.30): C, 66.26; H, 4.32; Found: C, 66.33; H, 4.26.

Anchoring of (8-hydroxy-9,10-dioxo-9,10-dihydro-anthracen-1-yloxy)-acetic acid ethyl ester on aminopropyl multi-wall carbon nanotube (APSiO₂-MWCNT)

Aminopropyl multi wall carbon nanotube (APSiO₂-MWCNT) (1.0 g) was added to a solution of (4-hydroxy-9,10-dioxo-9,10-dihydro-anthracen-1-yloxy)-acetic acid ethyl ester (2 mmol, 0.65 g) in absolute EtOH (30 mL) and the mixture was stirred under reflux for 48 h. Then the resulting mixture was centrifuged several times with ethanol and acetone in order to remove any physisorbed ligand. The heterogeneous ligand [AQ@APSiO₂-MWCNT] was isolated as a black powder.

Bis 1,8-mono ester hydroxy anthraquinone palladium (II) aminopropyl multi-wall carbon nanotube [AQ₂Pd(II)@APSiO₂-MWCNT]

[AQ@APSiO₂-MWCNT] (1.0 g) was added to a solution of Pd(OAc)₂ (1.0 mmol) in DMSO (30 mL) and the solution was reflux for 12 h. Then the resulting mixture was centrifuged several times with ethanol and water in order to remove any physisorbed palladium. The heterogeneous palladium catalyst [AQ₂Pd(II)@APSiO₂-MWCNT] was isolated as a black powder.

Determination of the palladium content in catalyst [AQ₂Pd(II)@APSiO₂-MWCNT]

In a screw-capped vessel, 100 mg of [AQ₂Pd(II)@APSiO₂-MWCNT] was extracted with (5 × 2 mL) concentrated HCl. then in order to digest the metal, 2 mL of concentrated nitric acid was added. The mixture was then transferred to a 100-mL volumetric flask, diluted (1:50) for the second time and submitted to ICP analysis. The palladium concentration was determined by measuring the atomic emission (340.46 nm) with reference to a linear ($R = 0.99$) calibration curve of (1–4 ppm) [AQ₂Pd(II)@APSiO₂-MWCNT] prepared in a manner identical to the sample preparation.

General procedure for deprotection of allyl, propargyl, and benzyl phenol derivatives in the presence of a catalytic amount of [(AQ)₂Pd(II)@APSiO₂-MWCNT]

According to the ICP results, the palladium content in the heterogeneous catalyst was determined to be 2.07 % (W/W).

Therefore, each gram of heterogeneous catalyst includes 2.73×10^{-4} mmol of palladium and 0.05 mmol of heterogeneous catalyst is equal to 0.183 g of the heterogeneous catalyst.

In a uncapped vial, a mixture of protected phenols (1.0 mmol), tetrabutylammonium bromide (TBAB) (0.5 g) and Cs₂CO₃ (1.1 mmol) was mixed and stirred in the presence of the catalytic amount (5.0 mol%) of [(AQ)₂Pd(II)@APSiO₂-MWCNT] at 100 °C. After the completion of the reaction (Table 2) as monitored by TLC, the mixture was diluted by EtOAc (10 mL), then the reaction mixture was centrifuged and the supernatant was decanted to separate the heterogeneous catalyst, which was washed several times with ethanol. Then the resulting mixture was extracted by continuous extraction with EtOAc (5 mL). The organic phase was separated and dried over anhydrous Na₂SO₄ which after filtration and evaporation of the solvent followed by purification on silica gel afforded the pure deprotected phenol derivatives.

2-(Prop-2-ynyloxy)naphthalene (1b) white crystal. mp = 57–58 °C. $R_f = 0.80$ (80 % *n*-Hexane: 20 % EtOAc). IR (KBr) $\nu = 3278.8, 3039.6, 2106.1, 1612.4, 1589.2, 1458.1, 1357.8, 1257.5, 1164.9, 1010.6, 941.2, 825.5, 748.3, 671.2, 470.6$ cm⁻¹. ¹H NMR (250 MHz, CDCl₃) $\delta = 2.66$ (t, $J = 2.4$ Hz, 1H), 2.84 (d, $J = 2.4$ Hz, 2H), 7.30–7.34 (m, 2H), 7.48–7.58 (m, 2H), 7.83–7.90 (m, 3H) ppm. ¹³C NMR (62.9 MHz, CDCl₃) $\delta = 53.63, 74.02, 76.80, 105.41, 116.72, 122.06, 124.54, 125.02, 125.76, 127.31, 127.66, 132.35, 153.47$ ppm. MS: m/z (%) = 183 (7.8, $M^+ + 1$), 182 (8.9, M^+), 147 (15.8), 129 (11.7), 111 (30.4), 97 (32.3), 85 (42.1), 69 (60.8), 57 (100.0). Anal. Calcd for C₁₃H₁₀O (182.22): C, 85.69; H, 5.53; found: C, 85.67; H, 5.54.

1-(Prop-2-ynyloxy)-9H-xanthen-9-one (1d) white crystal. mp = 166–167 °C. $R_f = 0.23$ (80 % *n*-Hexane: 20 % EtOAc). IR (KBr) $\nu = 3217.0, 2106.1, 1658.7, 1604.7, 1558.4, 1473.5, 1288.4, 1234.3, 1072.3, 918.1$ cm⁻¹. ¹H NMR (250 MHz, CDCl₃) $\delta = 2.55$ (s, 1H), 4.90 (s, 2H), 6.94 (d, $J = 8.2$ Hz, 1H), 7.08 (d, $J = 8.2$ Hz, 1H), 7.27–7.38 (m, 2H), 7.54–7.66 (m, 2H), 8.26 (d, $J = 7.9$ Hz, 1H) ppm. ¹³C NMR (62.9 MHz, CDCl₃) $\delta = 57.09, 76.40, 78.00, 108.03, 111.22, 117.24, 122.88, 123.85, 126.75, 134.24, 134.50, 154.95, 158.02, 158.26, 177.00$ ppm. MS: m/z (%) = 252 (3.1, $M^+ + 2$), 251 (51.5, $M^+ + 1$), 250 (60.8, M^+), 221 (100.0), 196 (93.1), 168 (83.8), 155 (46.0), 139 (62.5), 127 (80.1), 101 (26.8), 69 (83.2), 57 (69.1). Anal. Calcd for C₁₆H₁₀O₃ (250.25): C, 76.79; H, 4.03; found: C, 76.80; H, 4.12.

4-Methyl-7,8-bis(prop-2-ynyloxy)-2H-chromen-2-one (1g) cream crystal. mp = 124–125 °C. $R_f = 0.64$ (EtOAc). IR (KBr) $\nu = 3267.5, 2109.8, 1725.7, 1589.6, 1566.1, 1203.5, 1121.6, 979.8, 841.9, 786.9$ cm⁻¹. ¹H NMR (250 MHz, CDCl₃) $\delta = 2.32$ (s, 3H), 2.38 (t, $J = 2.5$ Hz, 1H), 2.50 (t, $J = 2.5$ Hz, 1H), 4.78 (d, $J = 2.5$ Hz, 2H), 4.79 (d, $J = 2.5$ Hz, 2H), 6.07 (s, 1H), 6.97 (d, $J = 8.7$ Hz, 1H),

7.28 (d, $J = 8.7$ Hz, 1H). ^{13}C NMR (62.9 MHz, CDCl_3) $\delta = 18.74, 57.08, 60.55, 76.27, 76.62, 77.71, 78.14, 110.15, 112.69, 115.37, 120.17, 132.50, 152.55, 153.43, 160.13, 166.78$. MS: m/z (%) = 270 (4.4, $\text{M}^+ + 2$), 269 (21.4, $\text{M}^+ + 1$), 268 (26.7, M^+), 230 (100.0), 145 (20.4), 106 (33.3), 78 (46.4), 69 (30.1). Anal. Calcd for $\text{C}_{16}\text{H}_{12}\text{O}_4$ (268.26): C, 71.64; H, 4.51; found: C, 71.34; H, 4.10.

4-Chloro-2-nitro-1-(prop-2-ynyloxy)benzene (1i) pale yellow crystal. mp = 73–74 °C. $R_f = 0.56$ (80 % *n*-Hexane: 20 % EtOAc). IR (KBr) $\nu = 3294.2, 3085.9, 2916.2, 2129.3, 1620.1, 1481.2, 1257.5, 1126.3, 995.2, 848.6, 686.6$ cm^{-1} . ^1H NMR (250 MHz, CDCl_3) $\delta = 2.61$ (t, $J = 2.5$ Hz, 1H), 4.82 (d, $J = 2.5$ Hz, 2H), 7.22 (s, 1H), 7.49 (dd, $J_1 = 9.0, J_2 = 2.7$ Hz, 1H), 7.80 (d, $J = 2.7$ Hz, 1H). ^{13}C NMR (62.9 MHz, CDCl_3) $\delta = 57.50, 76.80, 77.69, 116.89, 125.49, 126.30, 133.87, 140.21, 149.41$. MS: m/z (%) = 212 (0.4, $\text{M}^+ + 1$), 211 (0.4, M^+), 183.0 (1.1), 149 (12.1), 111 (14.6), 97 (24.8), 85 (32.0), 71 (50.6), 57 (100.0). Anal. Calcd for $\text{C}_9\text{H}_6\text{ClNO}_3$ (211.60): C, 51.08; H, 2.86; Cl, 16.75; N, 6.62; found: C, 51.01; H, 2.88; Cl, 16.83; N, 6.60.

4-Allyl-2-methoxy-1-(prop-2-ynyloxy)benzene (1k) colorless oil. $R_f = 0.83$ (80 % *n*-Hexane: 20 % EtOAc). IR (neat) $\nu = 3253.0, 3046.5, 2951.9, 2120.0, 1640.4, 1579.8, 1521.7, 1458.6, 1419.5, 1265.2, 1228.2, 1140.3, 1018.3, 990.6, 918.4$ cm^{-1} . ^1H NMR (250 MHz, CDCl_3) $\delta = 2.46$ (t, $J = 2.4$ Hz, 1H), 3.25 (d, $J = 6.7$ Hz, 2H), 3.72 (s, 3H), 4.60 (d, $J = 2.4$ Hz, 2H), 4.98–5.09 (m, 2H), 5.80–5.97 (m, 1H), 6.61–6.65 (m, 2H), 6.86 (d, $J = 8.3$ Hz, 1H). ^{13}C NMR (62.9 MHz, CDCl_3) $\delta = 39.64, 55.44, 56.68, 75.81, 79.01, 112.40, 114.92, 115.52, 120.21, 133.93, 137.55, 145.17, 149.74$. MS: m/z (%) = 203 (9.6, $\text{M}^+ + 1$), 202 (20.0, M^+), 163.0 (100.0), 107 (33.9), 103 (69.6), 91 (87.8), 77 (66.1), 65 (40.0), 55 (45.2); Anal. Calcd for $\text{C}_{13}\text{H}_{14}\text{O}_2$ (202.25): C, 77.20; H, 6.98; found: C, 77.34; H, 7.05.

2-Allyl-1-(prop-2-ynyloxy)anthracene-9,10-dione (1l) yellow crystal. mp = 119–120 °C. $R_f = 0.63$ (80 % *n*-Hexane: 20 % EtOAc). IR (KBr) $\nu = 3255.6, 3070.5, 2939.3, 2113.8, 1666.4, 1566.1, 1458.1, 1411.8, 1319.2, 1249.8, 1188.1, 1026.1, 956.6, 709.8, 570.9$ cm^{-1} . ^1H NMR (250 MHz, CDCl_3) $\delta = 2.52$ (t, $J = 2.5$ Hz, 1H), 3.59 (d, $J = 6.7$ Hz, 2H), 4.76 (d, $J = 2.5$ Hz, 2H), 5.06–5.13 (m, 2H), 5.79–5.90 (m, 1H), 7.53 (d, $J = 8.0$ Hz, 1H), 7.61–7.65 (m, 2H), 7.95 (d, $J = 8.0$ Hz, 1H), 8.03–8.10 (m, 2H). ^{13}C NMR (62.9 MHz, CDCl_3) $\delta = 34.62, 61.56, 76.11, 79.14, 117.25, 123.92, 125.59, 126.46, 126.86, 132.34, 133.47, 133.78, 134.01, 134.41, 135.52, 135.56, 143.18, 155.95, 182.31, 182.49$. MS: m/z (%) = 303 (3.0, $\text{M}^+ + 1$), 302 (10.8, M^+), 284.0 (13.2), 263 (100.0), 274 (7.8), 237 (45.5), 202 (11.8), 178 (30.7), 152 (20.1), 129 (13.8), 105 (22.3), 73 (47.4), 57 (96.8). Anal. Calcd for $\text{C}_{20}\text{H}_{14}\text{O}_3$ (302.32): C, 79.46; H, 4.67; found: C, 79.44; H, 4.57.

2-Allyl-1-hydroxy-anthraquinone (2l) yellow crystal; mp = 115–116 °C; $R_f = 0.90$ (50 % *n*-Hexane: 50 % EtOAc); IR

(KBr) $\nu = 3448.5, 1666.4, 1635.5, 1589.2, 1427.2, 1357.8, 1296.1, 1265.2, 1226.6, 1002.9, 918.1, 766.0, 709.8$ cm^{-1} ; ^1H NMR (250 MHz, CDCl_3) $\delta = 3.49$ (d, $J = 6.6$ Hz, 2H), 5.11–5.19 (m, 2H), 5.93–6.09 (m, 1H), 7.50 (dd, $J_1 = 7.7$ Hz, $J_2 = 0.6$ Hz, 1H), 7.63–7.79 (m, 3H), 8.19–8.27 (m, 2H), 12.9 (s, 1H); ^{13}C NMR (62.9 MHz, CDCl_3) $\delta = 33.77, 115.39, 117.10, 119.26, 124.28, 126.81, 127.24, 131.52, 133.16, 133.64, 134.10, 134.51, 134.82, 136.37, 160.50, 182.16, 188.79$; MS: m/z (%) = 266 (4.8, $\text{M}^+ + 2$), 265 (61.7, $\text{M}^+ + 1$), 264 (100.0, M^+), 249 (36.7), 189 (37.8), 152 (36.7), 105 (28.7), 81 (36.2), 69 (79.8), 57 (71.8). Anal. Calcd for $\text{C}_{17}\text{H}_{12}\text{O}_3$ (264.28): C, 77.26; H, 4.58; found: C, 77.30; H, 4.52.

Ethyl-2-(9,10-dioxo-4-(prop-2-ynyloxy)-9,10-dihydroanthracen-1-yloxy)acetate (1m) yellow crystal. mp = 115–116 °C. $R_f = 0.60$ (50 % *n*-Hexane: 50 % EtOAc). IR (KBr) $\nu = 3294.2, 1743.5, 1666.4, 1573.8, 1458.1, 1404.1, 1319.2, 1249.8, 1211.2, 1056.9, 995.2, 810.0, 725.2$ cm^{-1} . ^1H NMR (250 MHz, CDCl_3) $\delta = 1.21$ (t, $J = 7.2$ Hz, 3H), 2.51 (t, $J = 2.4$ Hz, 1H), 4.19 (q, $J = 7.2$ Hz, 2H), 7.71 (s, 2H), 4.79 (d, $J = 2.4$ Hz, 2H), 7.26 (d, $J = 9.3$ Hz, 1H), 7.40 (d, $J = 7.6$ Hz, 1H), 7.59–7.65 (m, 2H), 8.01–8.08 (m, 2H). ^{13}C NMR (62.9 MHz, CDCl_3) $\delta = 14.12, 58.01, 61.36, 67.91, 76.71, 78.12, 123.50, 123.81, 124.32, 124.48, 126.37, 126.40, 133.39, 133.41, 133.84, 133.89, 152.90, 153.15, 168.62, 182.56, 182.61$. MS: m/z (%) = 366 (2.1, $\text{M}^+ + 2$), 365 (3.6, $\text{M}^+ + 1$), 364 (7.0, M^+), 291 (25.4), 262 (22.7), 239 (40.0), 125 (15.7), 111 (31.4), 97 (43.4), 83 (40.7), 71 (60.3), 57 (100.0). Anal. Calcd for $\text{C}_{21}\text{H}_{16}\text{O}_6$ (364.35): C, 69.23; H, 4.43; found: C, 69.17; H, 4.37.

Ethyl-2-(9,10-dioxo-8-(prop-2-ynyloxy)-9,10-dihydroanthracen-1-yloxy)acetate (1n) yellow crystal. mp = 149–150 °C. $R_f = 0.55$ (50 % *n*-Hexane: 50 % EtOAc). IR (KBr) $\nu = 3294.2, 2993.3, 1743.5, 1666.4, 1589.2, 1442.7, 1380.9, 1319.2, 1288.4, 1211.2, 987.5, 740.6, 632.6$ cm^{-1} . ^1H NMR (250 MHz, CDCl_3) $\delta = 1.21$ (t, $J = 7.1$ Hz, 3H), 2.49 (t, $J = 2.4$ Hz, 1H), 4.19 (q, $J = 7.1$ Hz, 2H), 4.78 (s, 2H), 4.85 (d, $J = 2.4$ Hz, 2H), 7.14 (d, $J = 8.3$ Hz, 1H), 7.42 (d, $J = 8.3$ Hz, 1H), 7.49–7.61 (m, 3H), 7.83 (d, $J = 7.7$ Hz, 1H). ^{13}C NMR (62.9 MHz, CDCl_3) $\delta = 14.12, 57.21, 61.43, 66.85, 76.62, 77.98, 120.18, 120.45, 120.64, 120.98, 124.81, 133.70, 133.72, 134.70, 134.73, 157.09, 157.66, 168.49, 181.99, 183.36$. MS: m/z (%) = 364 (3.4, M^+), 325 (100.0), 297 (16.4), 277 (79.8), 253 (21.8), 236 (30.8), 224 (30.6), 167 (14.6), 139 (44.9), 97 (10.2), 57 (21.4). Anal. Calcd for $\text{C}_{21}\text{H}_{16}\text{O}_6$ (364.35): C, 69.23; H, 4.43; found: C, 69.12; H, 4.40.

Allyloxy-benzene (1o) $R_f = 0.72$ (80 % *n*-Hexane: 20 % EtOAc). ^1H NMR (250 MHz, CDCl_3) $\delta = 4.58$ –4.63 (m, 2H), 5.38 (dd, $J_1 = 10.4, J_2 = 1.3$ Hz, 1H), 5.52 (dd, $J_1 = 17.4, J_2 = 1.6$ Hz, 1H), 6.11–6.18 (m, 1H), 7.00–7.05 (m, 3H), 7.37–7.39 (m, 2H). ^{13}C NMR (62.9 MHz, CDCl_3) $\delta = 68.71, 114.79, 117.57, 120.90, 129.52, 133.47, 158.70$.

1-(Allyloxy)anthracene-9,10-dione (1p) yellow crystal. mp = 138–139 °C. $R_f = 0.30$ (80 % *n*-Hexane: 20 % EtOAc). IR (KBr) $\nu = 3001.0, 2923.9, 1666.4, 1573.8, 1442.7, 1319.2, 1265.2, 1226.6, 964.3, 702.0 \text{ cm}^{-1}$. $^1\text{H NMR}$ (250 MHz, CDCl_3) $\delta = 4.61$ (d, $J = 4.7$ Hz, 2H), 5.27 (dd, $J_1 = 10.6, J_2 = 1.3$ Hz, 1H), 5.57 (dd, $J_1 = 17.2, J_2 = 1.5$ Hz, 1H), 5.94–6.09 (m, 1H), 7.15 (d, $J = 7.9$ Hz, 1H), 7.47–7.63 (m, 3H), 7.76 (dd, $J_1 = 7.7, J_2 = 0.7$ Hz, 1H), 8.00–8.17 (m, 2H). $^{13}\text{C NMR}$ (62.9 MHz, CDCl_3) $\delta = 69.78, 118.03, 119.28, 119.76, 121.51, 126.40, 127.08, 132.07, 132.27, 133.07, 134.12, 134.70, 134.85, 135.51, 159.15, 181.90, 183.18$. MS: m/z (%) = 266 (0.6, $\text{M}^+ + 2$), 265 (20.9, $\text{M}^+ + 1$), 264 (45.8, M^+), 249 (33.7), 236 (73.7), 221 (55.9), 180 (81.6), 168 (25.7), 152 (64.0), 139 (100.0), 113 (23.4), 95 (17.4), 81 (40.2), 69 (91.7), 57 (51.6). Anal. Calcd for $\text{C}_{17}\text{H}_{12}\text{O}_3$ (264.28): C, 77.26; H, 4.58; found: C, 77.25; H, 4.63.

1,4-Bis(allyloxy)anthracene-9,10-dione (1q) dark orange crystal. mp = 104 °C. $R_f = 0.73$ (50 % *n*-Hexane: 50 % EtOAc). IR (KBr) $\nu = 1666.4, 1589.2, 1566.1, 1404.1, 1319.2, 1242.1, 1033.8, 979.8, 925.8, 802.3, 732.9, 640.3, 570.9 \text{ cm}^{-1}$. $^1\text{H NMR}$ (250 MHz, CDCl_3) $\delta = 4.43$ (d, $J = 4.8$ Hz, 4H), 5.15 (dd, $J_1 = 10.6, J_2 = 1.6$ Hz, 2H), 5.46 (dd, $J_1 = 17.2, J_2 = 1.7$ Hz, 2H), 5.84–5.99 (m, 2H), 7.01–7.05 (m, 2H), 7.46–7.49 (m, 2H), 7.90–7.94 (m, 2H). $^{13}\text{C NMR}$ (62.9 MHz, CDCl_3) $\delta = 70.33, 117.63, 121.81, 123.00, 126.15, 132.50, 133.02, 134.40, 152.97, 182.52$. MS: m/z (%) = 321 (1.2, $\text{M}^+ + 1$), 320 (1.5, M^+), 237 (4.1), 205 (8.7), 183 (3.9), 167 (5.5), 125 (17.4), 111 (31.2), 97 (46.7), 85 (43.1), 71 (63.4), 57 (100.0). Anal. Calcd for $\text{C}_{20}\text{H}_{16}\text{O}_4$ (320.34): C, 74.99; H, 5.03; found: C, 75.09; H, 5.12.

1,8-Bis(allyloxy)anthracene-9,10-dione (1r) yellow crystal. mp = 148–149 °C. $R_f = 0.46$ (80 % *n*-Hexane: 20 % EtOAc). IR (KBr) $\nu = 1666.4, 1581.5, 1442.7, 1319.2, 1288.4, 1234.4 \text{ cm}^{-1}$. $^1\text{H NMR}$ (250 MHz, CDCl_3) $\delta = 4.76$ (d, $J = 4.7$ Hz, 4H), 5.35 (dd, $J_1 = 10.6, J_2 = 1.6$ Hz, 2H), 5.62 (dd, $J_1 = 2.3, J_2 = 1.6$ Hz, 2H), 6.04–6.19 (m, 2H), 7.28 (dd, $J_1 = 8.5, J_2 = 1.0$ Hz, 2H), 7.59 (t, $J = 8.4$ Hz, 2H), 7.83 (dd, $J_1 = 8.8, J_2 = 1.1$ Hz, 2H). $^{13}\text{C NMR}$ (62.9 MHz, CDCl_3) $\delta = 70.02, 117.76, 119.18, 119.88, 124.54, 132.47, 133.59, 134.81, 158.30, 184.03$. MS: m/z (%) = 321 (10.4, $\text{M}^+ + 1$), 320 (14.1, M^+), 237 (11.0), 137 (10.9), 113 (15.9), 97 (50.8), 83 (48.3), 71 (48.2), 57 (100.0). Anal. Calcd for $\text{C}_{20}\text{H}_{16}\text{O}_4$ (320.34): C, 74.99; H, 5.03; found: C, 74.89; H, 5.00.

7,8-Bis(allyloxy)-4-methyl-2H-chromen-2-one (1s) cream crystal. mp = 50 °C. $R_f = 0.26$ (80 % *n*-Hexane: 20 % EtOAc). IR (KBr) $\nu = 3070.5, 2916.2, 1905.5, 1728.1, 1596.9, 1427.2, 1288.4, 1080.1, 979.8, 941.2, 624.9 \text{ cm}^{-1}$. $^1\text{H NMR}$ (250 MHz, CDCl_3) $\delta = 2.27$ (s, 3H), 4.57 (s, 4H), 5.07–5.38 (m, 4H), 5.98–6.05 (m, 2H), 6.77 (d, $J = 8.7$ Hz, 2H), 7.17 (d, $J = 8.7$ Hz, 1H). $^{13}\text{C NMR}$ (62.9 MHz, CDCl_3) $\delta = 18.54, 69.54, 74.28, 109.40, 111.95, 114.52, 117.66,$

118.00, 119.58, 132.42, 133.87, 134.70, 147.73, 152.75, 154.36, 160.33. MS: m/z (%) = 274 (3.5, $\text{M}^+ + 2$), 273 (11.2, $\text{M}^+ + 1$), 272 (13.8, M^+), 231 (47.7), 191 (42.8), 163 (27.6), 136 (19.3), 109 (19.9), 91 (48.3), 69 (100.0), 57 (95.9). Anal. Calcd for $\text{C}_{16}\text{H}_{16}\text{O}_4$ (272.30): C, 70.57; H, 5.92; found: C, 70.65; H, 6.03.

1-Allyloxy-4-methyl-benzene (1t) $R_f = 0.76$ (80 % *n*-Hexane: 20 % EtOAc). $^1\text{H NMR}$ (250 MHz, CDCl_3) $\delta = 2.28$ (s, 3H), 4.49–4.53 (m, 2H), 5.27 (dd, $J_1 = 10.5, J_2 = 1.5$ Hz, 1H), 5.40 (dd, $J_1 = 17.4, J_2 = 1.6$ Hz, 1H), 5.98–6.11 (m, 1H), 6.80–6.83 (m, 2H), 7.06–7.09 (m, 2H). $^{13}\text{C NMR}$ (62.9 MHz, CDCl_3) $\delta = 20.25, 68.83, 114.28, 117.17, 129.63, 129.95, 133.95, 156.90$.

1-Allyloxy-4-nitro-benzene (1u) $R_f = 0.54$ (80 % *n*-Hexane: 20 % EtOAc). $^1\text{H NMR}$ (250 MHz, CDCl_3) $\delta = 4.57$ – –4.61 (m, 2H), 5.29 (dd, $J_1 = 10.4, J_2 = 1.4$ Hz, 1H), 5.39 (dd, $J_1 = 17.3, J_2 = 1.6$ Hz, 1H), 5.95–6.04 (m, 1H), 6.92 (dd, $J_1 = 8.3, J_2 = 1.0$ Hz, 2H), 8.09–8.14 (m, 2H). $^{13}\text{C NMR}$ (62.9 MHz, CDCl_3) $\delta = 69.35, 114.66, 118.48, 125.78, 129.82, 131.91, 163.59$.

4-Allyl-1-(allyloxy)-2-methoxybenzene (1v) colorless oil. $R_f = 0.81$ (80 % *n*-Hexane: 20 % EtOAc). IR (neat) $\nu = 3070.5, 2923.9, 1843.8, 1643.2, 1589.2, 1512.1, 1458.1, 1419.5, 1265.2, 1226.6, 1149.5, 1018.3, 995.2, 918.1, 802.3, 748.3 \text{ cm}^{-1}$. $^1\text{H NMR}$ (250 MHz, CDCl_3) $\delta = 0.02$ –0.06 (m, 2H), 3.54 (s, 3H), 4.24–4.27 (m, 2H), 4.77–4.99 (m, 2H), 5.08–5.16 (m, 2H), 5.00–5.81 (m, 2H), 6.38–6.54 (m, 3H). $^{13}\text{C NMR}$ (62.9 MHz, CDCl_3) $\delta = 39.62, 55.42, 69.61, 112.43, 113.84, 115.24, 116.80, 120.29, 132.76, 133.73, 137.63, 146.53, 149.58$. MS: m/z (%) = 205 (4.0, $\text{M}^+ + 1$), 204 (9.0, M^+), 163 (100.0), 149 (29.0), 107 (42.0), 103 (75.0), 91 (93.0), 69 (20.0), 57 (75.0). Anal. Calcd for $\text{C}_{13}\text{H}_{16}\text{O}_2$ (204.26): C, 76.44; H, 7.90; found: C, 76.57; H, 7.84.

Ethyl 2-(4-(allyloxy)-9,10-dioxo-9,10-dihydroanthracen-1-yloxy)acetate (1w) yellow crystal. mp = 116 °C. $R_f = 0.55$ (50 % *n*-Hexane: 50 % EtOAc). IR (KBr) $\nu = 1735.8, 1666.4, 1581.5, 1450.4, 1396.4, 1319.2, 1249.8, 1211.2, 987.5, 810.0, 725.2 \text{ cm}^{-1}$. $^1\text{H NMR}$ (250 MHz, CDCl_3) $\delta = 1.21$ (t, $J = 7.1$ Hz, 3H), 4.19 (q, $J = 7.1$ Hz, 2H), 4.61 (d, $J = 7.1$ Hz, 2H), 4.69 (s, 2H), 5.27 (dd, $J_1 = 10.5, J_2 = 1.5$ Hz, 1H), 5.53 (dd, $J_1 = 17.2, J_2 = 1.7$ Hz, 1H), 5.96–6.11 (m, 1H), 7.19 (d, $J = 9.2$ Hz, 1H), 7.25 (d, $J = 9.2$ Hz, 1H), 7.60–7.64 (m, 2H), 8.03–8.11 (m, 2H). $^{13}\text{C NMR}$ (62.9 MHz, CDCl_3) $\delta = 14.14, 61.34, 68.28, 70.53, 118.06, 121.57, 123.26, 124.69, 126.39, 126.42, 132.36, 133.24, 133.42, 133.87, 134.12, 152.24, 154.49, 168.81, 182.64, 182.90$. MS: m/z (%) = 368 (0.7, $\text{M}^+ + 2$), 367 (1.5, $\text{M}^+ + 1$), 366 (1.5, M^+), 323 (1.6), 293 (4.2), 275 (2.4), 256 (2.8), 239 (5.3), 205 (5.5), 184 (4.9), 160 (4.5), 137 (6.9), 111 (21.5), 97 (29.3), 83 (34.7), 69 (60.5), 57 (100.0). Anal. Calcd for $\text{C}_{21}\text{H}_{18}\text{O}_6$ (366.36): C, 68.85; H, 4.95; found: C, 68.87; H, 4.90.

Ethyl 2-(8-(allyloxy)-9,10-dioxo-9,10-dihydroanthracen-1-yloxy)acetate (1x) yellow crystal. mp = 90–91 °C. R_f = 0.50 (50 % *n*-Hexane: 50 % EtOAc). IR (KBr) ν = 2993.3, 1743.5, 1666.4, 1589.2, 1434.9, 1380.9, 1319.2, 1234.3, 1203.5, 1072.8, 740.6, 663.5, 586.3 cm^{-1} . ^1H NMR (250 MHz, CDCl_3) δ = 0.91 (t, J = 7.2 Hz, 3H), 3.88 (q, J = 7.2 Hz, 2H), 4.34 (d, J = 4.5 Hz, 2H), 4.50 (s, 2H), 4.95 (dd, J_1 = 10.5, J_2 = 1.5 Hz, 1H), 5.25 (dd, J_1 = 17.2, J_2 = 1.5 Hz, 1H), 5.66–5.81 (m, 1H), 6.87 (d, J = 8.2 Hz, 1H), 7.12 (d, J = 8.0 Hz, 1H), 7.17 (d, J = 2.5 Hz, 1H), 7.21 (d, J = 8.2 Hz, 1H), 7.34 (dd, J_1 = 7.7, J_2 = 0.7 Hz, 1H), 7.44 (dd, J_1 = 7.5, J_2 = 0.7 Hz, 1H). ^{13}C NMR (62.9 MHz, CDCl_3) δ = 13.99, 61.16, 66.72, 69.66, 117.53, 118.76, 119.57, 120.09, 120.67, 123.76, 124.71, 132.36, 133.41, 133.62, 134.35, 134.49, 157.42, 158.06, 168.37, 181.52, 183.15. MS: m/z (%) = 367 (1.6, M^+), 366 (4.5, M^+), 322 (5.5), 279 (9.7), 251 (6.9), 224 (7.1), 196 (3.58), 180 (4.4), 155 (6.1), 139 (11.4), 111 (28.4), 97 (35.9), 83 (36.4), 71 (67.0), 57 (100.0). Anal. Calcd for $\text{C}_{21}\text{H}_{18}\text{O}_6$ (366.36): C, 68.85; H, 4.95; found: C, 68.78; H, 5.02.

4-(Allyloxy)benzaldehyde (1y) colorless oil. R_f = 0.66 (80 % *n*-Hexane: 20 % EtOAc). IR (neat) ν = 3078.2, 2846.7, 2746.4, 1689.5, 1589.2, 1504.4, 1427.2, 1311.5, 1265.2, 1164.9, 1110.9, 1002.9, 933.5, 825.5, 655.8, 594.0, 509.2 cm^{-1} . ^1H NMR (250 MHz, CDCl_3) δ = 4.27–4.31 (m, 2H), 4.97–5.18 (m, 2H), 5.66–5.83 (m, 1H), 6.50–6.74 (m, 2H), 7.46–7.54 (m, 2H), 9.57 (s, 1H). ^{13}C NMR (62.9 MHz, CDCl_3) δ = 68.52, 114.16, 117.61, 129.78, 131.50, 132.31, 163.17, 190.13. MS: m/z (%) = 163 (7.5, M^+), 162 (51.6, M^+), 121 (66.0), 105 (56.0), 81 (47.2), 77 (59.7), 65 (100.0), 57 (78.0). Anal. Calcd for $\text{C}_{10}\text{H}_{10}\text{O}_2$ (162.19): C, 74.06; H, 6.21; found: C, 74.11; H, 6.20.

Benzyloxy-benzene (1z) R_f = 0.63 (80 % *n*-Hexane: 20 % EtOAc). ^1H NMR (250 MHz, CDCl_3) δ = 5.32 (s, 2H), 7.31–7.38 (m, 3H), 7.62–7.79 (m, 7H). ^{13}C NMR (62.9 MHz, CDCl_3) δ = 70.11, 115.25, 121.32, 128.25, 128.45, 128.92, 129.90, 137.58, 159.29.

1-Benzyloxy-4-nitro-benzene (1ab) R_f = 0.51 (80 % *n*-Hexane: 20 % EtOAc). ^1H NMR (250 MHz, CDCl_3) δ = 5.16 (s, 2H), 6.99–7.06 (m, 2H), 7.34–7.46 (m, 5H), 8.16–8.22 (m, 2H). ^{13}C NMR (62.9 MHz, CDCl_3) δ = 70.68, 114.87, 125.93, 127.55, 128.52, 128.82, 135.54, 141.61, 163.72.

1-(Benzyloxy)anthracene-9,10-dione (1ac) yellow crystal. mp = 165–166 °C. R_f = 0.23 (80 % *n*-Hexane: 20 % EtOAc). IR (KBr) ν = 3047.3, 2931.6, 1666.4, 1573.8, 1442.7, 1311.5, 1265.2, 956.6, 702.0 cm^{-1} . ^1H NMR (250 MHz, CDCl_3) δ = 5.17 (s, 2H), 7.19–7.31 (m, 2H), 7.33 (t, J = 1.7 Hz, 1H), 7.46–7.53 (m, 1H), 7.58 (dd, J_1 = 7.5 Hz, J_2 = 1.5 Hz, 1H), 7.60 (d, J = 2.0 Hz, 1H), 7.65 (dd, J_1 = 7.2 Hz, J_2 = 1.7 Hz, 1H), 7.79 (dd, J_1 = 7.5 Hz, J_2 = 1.2 Hz, 1H), 8.06 (d, J = 1.7 Hz, 1H), 8.08–8.09 (m, 1H), 8.13–8.14 (m, 1H), 8.16 (d, J = 1.7 Hz,

1H). ^{13}C NMR (62.9 MHz, CDCl_3) δ = 70.91, 119.64, 120.01, 121.89, 126.50, 126.72, 127.20, 127.89, 128.68, 132.39, 133.15, 134.17, 134.77, 134.95, 135.66, 136.23, 159.15, 182.03, 183.30. MS: m/z (%) = 315 (5.3, M^+), 314 (13.8, M^+), 208 (1.4), 180 (2.3), 139 (4.7), 113 (1.4), 91 (100.0), 65 (13.8). Anal. Calcd for $\text{C}_{21}\text{H}_{14}\text{O}_3$ (314.33): C, 80.24; H, 4.49; found: C, 80.18; H, 4.37.

4-Allyl-1-(benzyloxy)-2-methoxybenzene (1ad) colorless oil. R_f = 0.80 (80 % *n*-Hexane: 20 % EtOAc). IR (neat) ν = 3047.3, 2931.6, 1635.5, 1596.9, 1504.4, 1458.1, 1380.9, 1265.2, 1226.6, 1141.8, 1033.8, 918.1, 1848.6, 1802.3, 740.6, 694.3 cm^{-1} . ^1H NMR (250 MHz, CDCl_3) δ = 3.18 (d, J = 6.7 Hz, 2H), 3.72 (s, 3H), 4.91–4.99 (m, 4H), 5.74–5.90 (m, 1H), 6.53 (dd, J_1 = 8.0 Hz, J_2 = 1.7 Hz, 1H), 6.60 (d, J = 2.0 Hz, 1H), 6.68 (d, J = 8.0 Hz, 1H), 6.13–6.31 (m, 5H). ^{13}C NMR (62.9 MHz, CDCl_3) δ = 39.95, 55.96, 71.22, 112.56, 114.38, 115.77, 120.57, 127.41, 127.85, 128.60, 133.35, 137.53, 137.77, 146.70, 149.79. MS: m/z (%) = 256 (1.4, M^+), 255 (7.6, M^+), 254 (8.6, M^+), 163 (12.0), 91 (100.0); Anal. Calcd for $\text{C}_{17}\text{H}_{18}\text{O}_2$ (254.32): C, 80.28; H, 7.13; found: C, 80.36; H, 7.10.

2-Allyl-1-benzyloxy-anthraquinone (1ae) yellow crystal. mp = 101–102 °C. R_f = 0.90 (50 % *n*-Hexane: 50 % EtOAc). IR (KBr) ν = 1951.8, 1743.5, 1666.4, 1566.1, 1458.1, 1319.2, 1242.1, 956.6, 918.1, 709.8 cm^{-1} . ^1H NMR (250 MHz, CDCl_3) δ = 3.39 (d, J = 6.5 Hz, 2H), 4.94 (s, 2H), 5.00–5.07 (m, 2H). ^{13}C NMR (62.9 MHz, CDCl_3) δ = 24.45, 69.72, 76.24, 78.09, 117.29, 123.70, 126.64, 127.32, 128.25, 128.48, 128.89, 132.63, 133.52, 134.16, 134.82, 135.60, 135.81, 137.05, 142.89, 157.27, 182.62, 183.09. MS: m/z (%) = 356 (0.1, M^+), 355 (0.5, M^+), 354 (1.0, M^+), 336 (0.8), 263 (9.6), 250 (5.2), 237 (2.5), 219 (0.8), 178 (1.8), 149 (3.2), 117 (12.0), 91 (100.0), 57 (15.7). Anal. Calcd for $\text{C}_{24}\text{H}_{18}\text{O}_3$ (354.40): C, 81.34; H, 5.12; found: C, 81.27; H, 5.08.

Ethyl 2-(4-(benzyloxy)-9,10-dioxo-9,10-dihydroanthracen-1-yloxy)acetate (1af) yellow crystal. mp = 139–140 °C. R_f = 0.45 (50 % *n*-Hexane: 50 % EtOAc). IR (KBr) ν = 1743.5, 1666.4, 1566.1, 1450.4, 1396.4, 1249.8, 1203.5, 1072.3, 987.5, 725.2 cm^{-1} . ^1H NMR (250 MHz, CDCl_3) δ = 1.20 (t, J = 7.1 Hz, 3H), 4.18 (q, J = 7.1 Hz, 2H), 4.67 (s, 2H), 5.17 (s, 2H), 7.26 (t, J = 1.5 Hz, 1H), 7.29–7.32 (m, 2H), 7.35 (t, J = 1.5 Hz, 1H), 7.47–7.51 (m, 2H), 7.60–7.63 (m, 2H), 8.05–8.12 (m, 3H). ^{13}C NMR (62.9 MHz, CDCl_3) δ = 14.16, 61.40, 68.33, 71.77, 122.04, 124.64, 124.89, 126.50, 126.53, 126.95, 127.95, 128.67, 133.31, 133.47, 133.97, 134.20, 136.34, 152.46, 154.45, 168.82, 182.90, 182.98. MS: m/z (%) = 417 (1.1, M^+), 416 (8.1, M^+), 152 (3.4), 138 (3.9), 111 (8.0), 91 (100.0), 83 (16.4), 69 (21.0), 57 (36.6); Anal. Calcd for $\text{C}_{25}\text{H}_{20}\text{O}_6$ (416.42): C, 72.11; H, 4.84; found: C, 72.15; H, 4.97.

(8-Benzyloxy-9,10-dioxo-9,10-dihydro-anthracen-1-yloxy)-acetic acid ethyl ester (1ag) yellow crystal. mp =

143–144 °C. $R_f = 0.60$ (50 % *n*-Hexane: 50 % EtOAc). IR (KBr) $\nu = 1735.8, 1674.1, 1589.2, 1442.7, 1380.9, 1319.2, 1211.2 \text{ cm}^{-1}$. $^1\text{H NMR}$ (250 MHz, CDCl_3) $\delta = 1.27$ (t, $J = 7.0 \text{ Hz}$, 3H), 4.26 (q, $J = 7.0 \text{ Hz}$, 2H), 4.85 (s, 2H), 5.32 (s, 2H), 7.24–7.38 (m, 5H), 7.51–7.60 (m, 4H), 7.81 (dd, $J_1 = 7.7 \text{ Hz}$, $J_2 = 1.0 \text{ Hz}$, 1H), 7.90 (dd, $J_1 = 7.7 \text{ Hz}$, $J_2 = 1.0 \text{ Hz}$, 1H). $^{13}\text{C NMR}$ (62.9 MHz, CDCl_3) $\delta = 14.16, 61.44, 67.03, 70.95, 119.30, 120.15, 120.53, 120.84, 124.41, 125.10, 126.84, 127.77, 128.59, 133.62, 133.82, 134.71, 134.84, 136.45, 157.65, 158.25, 182.07, 183.58$. MS: m/z (%) = 418 (0.2, $\text{M}^+ + 2$), 417 (2.6, $\text{M}^+ + 1$), 416 (3.5, M^+), 329 (15.3), 253 (15.7), 224 (12.8), 139 (11.3), 111 (10.2), 91 (100.0), 57 (42.9). Anal. Calcd for $\text{C}_{25}\text{H}_{20}\text{O}_6$ (416.42): C, 72.11; H, 4.84; found: C, 72.24; H, 4.80.

1-(Allyloxy)-4-(prop-2-ynyloxy)anthracene-9,10-dione (**1ah**) yellow crystal. mp = 114–115 °C. $R_f = 0.76$ (50 % *n*-Hexane: 50 % EtOAc). IR (KBr) $\nu = 3217.0, 2106.1, 1666.4, 1566.1, 1458.1, 1411.8, 1319.2, 1249.8, 1033.8, 979.8, 918.1, 802.3, 725.2, 563.2 \text{ cm}^{-1}$. $^1\text{H NMR}$ (250 MHz, CDCl_3) $\delta = 2.54$ (t, $J = 2.4 \text{ Hz}$, 1H), 4.65 (d, $J = 4.8 \text{ Hz}$, 1H), 4.80 (d, $J = 2.4 \text{ Hz}$, 2H), 5.31 (dd, $J_1 = 10.5 \text{ Hz}$, $J_2 = 1.5 \text{ Hz}$, 1H), 5.57 (dd, $J_1 = 17.2 \text{ Hz}$, $J_2 = 1.6 \text{ Hz}$, 1H), 5.99–6.15 (m, 1H), 7.24 (d, $J = 7.9 \text{ Hz}$, 1H), 7.41 (d, $J = 9.4 \text{ Hz}$, 1H), 7.62–7.66 (m, 2H), 8.06–8.11 (m, 2H). $^{13}\text{C NMR}$ (62.9 MHz, CDCl_3) $\delta = 58.11, 70.29, 76.88, 78.41, 117.83, 121.34, 122.98, 124.04, 124.28, 126.18, 126.25, 132.37, 133.11, 133.27, 133.73, 133.92, 151.53, 154.00, 182.37, 182.70$. MS: m/z (%) = 320 (1.1, $\text{M}^+ + 2$), 319 (3.3, $\text{M}^+ + 1$), 318 (11.5, M^+), 279 (36.6), 249 (20.1), 221 (21.3), 193 (15.6), 165 (37.7), 127 (22.8), 111 (26.3), 97 (43.1), 71 (64.3), 57 (100.0). Anal. Calcd for $\text{C}_{20}\text{H}_{14}\text{O}_4$ (318.32): C, 75.46; H, 4.43; found: C, 75.50; H, 4.41.

1-(Allyloxy)-4-hydroxyanthracene-9,10-dione (**2r**) dark red crystal. mp = 124 °C. $R_f = 0.43$ (80 % *n*-Hexane: 20 % EtOAc). IR (KBr) $\nu = 3417.6, 2931.6, 1666.4, 1635.5, 1589.2, 1458.1, 1350.1, 1234.3, 1164.9, 995.2 \text{ cm}^{-1}$. $^1\text{H NMR}$ (250 MHz, CDCl_3) $\delta = 4.65$ (d, $J = 4.9 \text{ Hz}$, 2H), 5.31 (dd, $J_1 = 10.5 \text{ Hz}$, $J_2 = 1.5 \text{ Hz}$, 1H), 5.57 (dd, $J_1 = 17.2 \text{ Hz}$, $J_2 = 1.6 \text{ Hz}$, 1H), 6.00–6.15 (m, 1H), 7.19 (d, $J = 9.4 \text{ Hz}$, 1H), 7.30 (d, $J = 9.4 \text{ Hz}$, 1H), 7.64–7.76 (m, 2H), 8.15–8.21 (m, 2H), 12.92 (s, 1H). $^{13}\text{C NMR}$ (62.9 MHz, CDCl_3) $\delta = 70.41, 115.58, 117.87, 119.26, 125.39, 125.91, 126.08, 127.05, 131.91, 132.46, 133.02, 134.50, 134.65, 152.91, 157.31, 180.70, 188.43$. MS: m/z (%) = 281 (1.1, $\text{M}^+ + 1$), 280 (2.2, M^+), 236 (3.4), 209 (2.8), 191 (3.9), 179 (3.8), 165 (6.5), 149 (7.3), 125 (18.1), 111 (30.1), 97 (42.3), 83 (36.5), 71 (55.4), 57 (100.0). Anal. Calcd for $\text{C}_{17}\text{H}_{12}\text{O}_4$ (280.27): C, 72.85; H, 4.32; found: C, 72.92; H, 4.27.

1-(Benzyloxy)-4-(prop-2-ynyloxy)anthracene-9,10-dione (**1ai**) yellow crystal. mp = 142–143 °C. $R_f = 0.66$ (50 % *n*-Hexane: 50 % EtOAc). IR (KBr) $\nu = 3240.2, 2113.8, 1666.4, 1573.8, 1458.1, 1404.1, 1319.2, 1249.8, 1226.6,$

$1033.8, 979.8, 725.2, 694.3 \text{ cm}^{-1}$. $^1\text{H NMR}$ (250 MHz, CDCl_3) $\delta = 2.46$ (t, $J = 2.5 \text{ Hz}$, 1H), 4.69 (d, $J = 2.25 \text{ Hz}$, 2H), 5.1 (s, 2H), 7.15–7.18 (m, 1H), 7.21 (t, $J = 1.5 \text{ Hz}$, 1H), 7.24–7.30 (m, 2H), 7.44–7.47 (m, 2H), 7.53–7.56 (m, 2H), 7.98–8.04 (m, 3H). $^{13}\text{C NMR}$ (62.9 MHz, CDCl_3) $\delta = 58.25, 71.65, 76.66, 78.38, 121.89, 123.60, 124.15, 124.62, 126.40, 126.47, 126.92, 127.24, 127.90, 128.64, 133.28, 133.95, 134.12, 136.42, 151.86, 154.10, 182.71, 183.02$. MS: m/z (%) = 369 (1.2, $\text{M}^+ + 1$), 368 (4.0, M^+), 313 (2.3), 237 (12.1), 123 (22.0), 109 (25.4), 97 (43.9), 83 (46.2), 69 (57.8), 57 (100.0). Anal. Calcd for $\text{C}_{24}\text{H}_{16}\text{O}_4$ (368.38): C, 78.25; H, 4.38; found: C, 78.14; H, 4.23.

1-(Benzyloxy)-4-hydroxyanthracene-9,10-dione (**2s**) orange crystal. mp = 154–155 °C. $R_f = 0.43$ (80 % *n*-Hexane: 20 % EtOAc). IR (KBr) $\nu = 3433.1, 1666.4, 1635.5, 1589.2, 1450.4, 1427.2, 1350.1, 1234.3, 1157.2, 1010.6, 779.2, 725.2 \text{ cm}^{-1}$. $^1\text{H NMR}$ (250 MHz, CDCl_3) $\delta = 5.14$ (s, 2H), 7.25–7.31 (m, 3H), 7.33 (t, $J = 1.7 \text{ Hz}$, 1H), 7.48 (d, $J = 7.2 \text{ Hz}$, 1H), 7.60 (dd, $J_1 = 7.5 \text{ Hz}$, $J_2 = 1.5 \text{ Hz}$, 1H), 7.64 (d, $J = 9.0 \text{ Hz}$, 1H), 7.68 (dd, $J_1 = 7.5 \text{ Hz}$, $J_2 = 1.5 \text{ Hz}$, 1H), 8.11 (d, $J = 1.7 \text{ Hz}$, 1H), 8.14 (t, $J = 1.7 \text{ Hz}$, 1H), 8.18 (d, $J = 1.7 \text{ Hz}$, 1H), 12.87 (s, 1H). $^{13}\text{C NMR}$ (62.9 MHz, CDCl_3) $\delta = 71.87, 115.93, 126.07, 126.21, 126.31, 127.02, 127.33, 127.96, 128.66, 132.21, 133.24, 134.68, 134.93, 136.45, 152.98, 157.74, 181.29, 188.80$. MS: m/z (%) = 331 (0.8, $\text{M}^+ + 1$), 330 (2.1, M^+), 254 (1.9), 239 (2.1), 220 (1.9), 203 (2.1), 183 (3.1), 155 (3.8), 137 (6.2), 111 (18.4), 97 (31.5), 85 (34.9), 71 (60.9), 57 (100.0). Anal. Calcd for $\text{C}_{21}\text{H}_{14}\text{O}_4$ (330.33): C, 76.35; H, 4.27; found: C, 76.30; H, 4.21.

2-Prop-2-ynyloxy-benzoic acid prop-2-ynyl ester (**1aj**) yellow oil. $R_f = 0.55$ (50 % *n*-Hexane: 50 % EtOAc). IR (neat) $\nu = 3255.6, 2129.3, 1681.8, 1612.4, 1589.2, 1488.9, 1380.9, 1296.1, 1249.8, 1157.2, 1087.8 \text{ cm}^{-1}$. $^1\text{H NMR}$ (250 MHz, CDCl_3) $\delta = 2.44$ (t, $J = 2.5 \text{ Hz}$, 1H), 2.47 (t, $J = 2.5 \text{ Hz}$, 1H), 4.69 (d, $J = 2.2 \text{ Hz}$, 2H), 4.80 (d, $J = 2.2 \text{ Hz}$, 2H), 6.94 (t, $J = 7.5 \text{ Hz}$, 1H), 7.03 (d, $J = 8.2 \text{ Hz}$, 1H), 7.35–7.43 (m, 1H), 7.77 (dd, $J_1 = 7.7 \text{ Hz}$, $J_2 = 2.0 \text{ Hz}$, 1H). $^{13}\text{C NMR}$ (62.9 MHz, CDCl_3) $\delta = 52.30, 56.81, 75.06, 76.27, 77.84, 78.15, 114.43, 119.95, 121.31, 132.01, 133.82, 156.73, 164.76$. MS: m/z (%) = 216 (0.9, $\text{M}^+ + 2$), 215 (4.3, $\text{M}^+ + 1$), 214 (6.7, M^+), 175 (10.0), 159 (21.7), 133 (100.0), 121 (81.2), 92 (56.7), 77 (50.6), 57 (29.2). Anal. Calcd for $\text{C}_{13}\text{H}_{10}\text{O}_3$ (214.22): C, 72.89; H, 4.71; found: C, 72.96; H, 4.70.

2-Hydroxy-benzoic acid prop-2-ynyl ester (**2t**) white crystal. mp = 49–50 °C. $R_f = 0.025$ (*n*-Hexane). $^1\text{H NMR}$ (250 MHz, CDCl_3) $\delta = 2.48$ (t, $J = 2.4 \text{ Hz}$, 1H), 4.86 (d, $J = 2.4 \text{ Hz}$, 2H), 6.82 (t, $J = 7.2 \text{ Hz}$, 1H), 6.91 (dd, $J_1 = 8.4 \text{ Hz}$, $J_2 = 1.1 \text{ Hz}$, 1H), 7.39 (t, $J = 7.2 \text{ Hz}$, 1H), 7.80 (dd, $J_1 = 8.0 \text{ Hz}$, $J_2 = 1.7 \text{ Hz}$, 1H), 10.43 (s, 1H). $^{13}\text{C NMR}$ (62.9 MHz, CDCl_3) $\delta = 52.69, 75.77, 77.22, 111.77, 117.61, 119.26, 130.04, 136.09, 161.71, 169.24$. MS: m/z

(%) = 177 (6.3, M⁺+1), 176 (8.3, M⁺), 155 (11.1), 137 (18.3), 99 (27.8), 83 (40.9), 57 (100.0). Anal. Calcd for C₁₀H₈O₃ (176.17): C, 68.18; H, 4.58; found: C, 68.27; H, 4.49.

1,4-Dimethoxyanthracene-9,10-dione (1ak) yellow crystal. mp = 168–169 °C. *R*_f = 0.50 (EtOAc). IR (KBr) ν = 1674.1, 1589.2, 1566.1, 1465.8, 1404.1, 1326.9, 1242.1, 1188.1, 1049.2, 972.1, 725.2570.9 cm⁻¹. ¹H NMR (250 MHz, CDCl₃) δ = 8.37 (s, 6H), 7.21–7.23 (m, 2H), 7.56–7.63 (m, 2H), 8.01–8.06 (m, 2H). ¹³C NMR (62.9 MHz, CDCl₃) δ = 56.69, 120.03, 122.50, 126.12, 133.08, 133.93, 153.81, 182.94. MS: *m/z* (%) = 270 (1.8, M⁺+2), 269 (4.0, M⁺+1), 268 (10.4, M⁺), 239 (4.0), 209 (2.5), 193 (2.5), 165 (3.3), 137 (9.8), 111 (9.2), 81 (47.0), 69 (100.0). Anal. Calcd for C₁₆H₁₂O₄ (268.26): C, 71.64; H, 4.51; found: C, 71.60; H, 4.42.

1,3-Di(prop-2-ynyl)pyrimidine-2,4(1H,3H)-dione (1al) white crystal. mp = 101–102 °C. *R*_f = 0.75 (EtOAc). IR (KBr) ν = 3294.2, 3263.3, 3085.9, 2977.9, 2121.6, 1712.7, 1666.4, 1450.4, 1342.4, 1226.6, 802.3, 763.8, 686.6, 640.3, 563.2 cm⁻¹. ¹H NMR (250 MHz, CDCl₃) δ = 2.17 (t, *J* = 2.4 Hz, 1H), 2.51 (t, *J* = 2.6 Hz, 2H), 4.58 (d, *J* = 2.5 Hz, 2H), 4.68 (d, *J* = 2.5 Hz, 2H), 5.83 (d, *J* = 8.0 Hz, 1H). ¹³C NMR (62.9 MHz, CDCl₃) δ = 30.63, 38.26, 71.22, 76.06, 78.10, 78.26, 102.33, 141.53, 150.61, 161.92. MS: *m/z* (%) = 190 (1.2, M⁺+2), 189 (5.7, M⁺+1), 188 (30.7, M⁺), 149 (100.0), 121 (10.9), 96 (22.4), 71 (14.6), 52 (92.2). Anal. Calcd for C₁₀H₈N₂O₂ (188.18): C, 63.82; H, 4.28; N, 14.89; found: C, 63.81; H, 4.18; N, 14.72.

Acknowledgments We gratefully acknowledge the support of this work by the Shiraz University Research Council.

References

- Green TW, Wuts PGM (1999) Protective groups in organic synthesis. Wiley, New York
- Kocienski PJ (2004) Protecting groups. Georg Thieme Verlag, Stuttgart
- Schelhaas M, Waldmann H (1996) protecting group strategies in organic synthesis. Angew Chem Int Ed Engl 35:2056–2083. doi:10.1002/anie.199620561
- Crich D, Karatholuvhu MS (2008) Application of the 4-trifluoromethylbenzenepropargyl ether group as an unhindered, electron deficient protecting group for stereoselective glycosylation. J Org Chem 73:5173–5176. doi:10.1021/jo7023398
- Ishizaki M, Yamada M, Watanabe S, Hoshino O, Nishitani K, Hayashida M, Tanaka A, Hara H (2004) Palladium charcoal-catalyzed deprotection of *O*-allylphenols. Tetrahedron 60:7973–7981. doi:10.1016/j.tet.2004.05.097
- Weissman SA, Zewge D (2005) Recent advances in ether dealkylation. Tetrahedron 61:7833–7863. doi:10.1016/j.tet.2005.05.041
- Guibé F (1998) Allylic protecting groups and their use in a complex environment part II: allylic protecting groups and their removal through catalytic palladium 'TC-allyl' methodology. Tetrahedron 54:2967–3042. doi:10.1016/S0040-4020(97)10383-0
- Jobron L, Hindsgaul O (1999) Novel para-substituted benzyl ethers for hydroxyl group protection. J Am Chem Soc 121:5835–5836. doi:10.1021/ja9836085
- Pal M, Parasuraman K, Yelleswarapu KR (2003) Palladium-catalyzed cleavage of O/N-propargyl protecting groups in aqueous media under a copper-free condition I. Org Lett 5:349–352. doi:10.1021/ol027382t
- Diaz RR, Melgarejo CR, Espinosa MTPL, Cubero II (1994) A novel, mild, and practical regeneration of alcohols from their allylic ethers by NBS/H₂O. J Org Chem 59:7928–7929. doi:10.1021/jo00104a063
- Yadav JS, Chandrashekhar S, Sumita G, Kachake R (1996) Selective and unprecedented oxidative deprotection of allyl ethers with DDQ. Tetrahedron Lett 37:6603–6620. doi:10.1016/0040-4039(96)01478-5
- Espanet B, Dunach E, Perichon J (1992) SmCl₃-catalyzed electrochemical cleavage of allyl ethers. Tetrahedron Lett 33:2485–2488. doi:10.1016/S0040-4039(00)92221-4
- Kadam SM, Nayak SK, Banerji A (1992) Low-valent titanium: a new approach to deprotection of allyl and benzyl groups. Tetrahedron Lett 33:5129–5132. doi:10.1016/S0040-4039(00)61209-1
- Thomas RM, Mohan GH, Iyengar DS (1997) A novel, mild and facile reductive cleavage of allyl ethers by NaBH₄/I₂ system. Tetrahedron Lett 38:4721–4724. doi:10.1016/S0040-4039(97)01007-1
- Thomas RM, Reddy GS, Iyengar DS (1999) An efficient and selective deprotection of allyl ethers by a CeCl₃ · 7H₂O-NaI system. Tetrahedron Lett 40:7293–7294. doi:10.1016/S0040-4039(99)01575-0
- Punna S, Meunier S, Finn MG (2004) A hierarchy of aryloxide deprotection by boron tribromide. Org Lett 6:2777–2779. doi:10.1021/ol0489898
- Ohkubo M, Mochizuki S, Sano T, Kawaguchi Y, Okamoto S (2007) Selective cleavage of allyl and propargyl ethers to alcohols catalyzed by Ti(O-*i*-Pr)₄/MXn/Mg. Org Lett 9:773–776. doi:10.1021/ol062963u
- Yasuhara A, Kasano A, Sakamoto T (1999) An efficient method for the deallylation of allyl aryl ethers using electrochemically generated nickel. J Org Chem 64:4211–4213. doi:10.1021/jo9824706
- Vutukuri DR, Bharathi P, Yu Z, Rajasekaran K, Tran M-H, Thayumanavan S (2003) A mild deprotection strategy for allyl-protecting groups and its implications in sequence specific dendrimer synthesis. J Org Chem 68:1146–1149. doi:10.1021/jo026469p
- Tsukamoto H, Suzuki T, Kondo Y (2003) Facile removal strategy for allyl and allyloxycarbonyl protecting groups using solid-supported barbituric acid under palladium catalysis. Synlett 8:1105–1108. doi:10.1055/s-2003-39907
- Lee D-H, Lee YH, Harrowfield JM, Lee I-M, Lee HI, Lim WT, Kim Y, Jin M-J (2009) Phosphine-free sonogashira coupling: reactions of aryl halides catalyzed by palladium(II) complexes of azetidine-derived polyamines under mild conditions. Tetrahedron 65:1630–1634. doi:10.1016/j.tet.2008.12.032
- Srinivas K, Srinivas P, Prathima PS, Balaswamy K, Sridhar B, Rao MM (2012) Thiopseudourea ligated palladium complexes: synthesis, characterization and application as catalysts for Suzuki-Miyaura, Sonogashira, Heck and Hiyama reactions. Catal Sci Technol 2:1180–1187. doi:10.1039/C2CY00542E
- Garrett CE, Prasad K (2004) The art of meeting palladium specifications in active pharmaceutical ingredients produced by Pd-catalyzed reactions. Adv Synth Catal 346:889–900. doi:10.1002/adsc.200404071
- Rao CNR, Govindaraj A (2002) Carbon nanotubes from organometallic precursors. Acc Chem Res 35:998–1007. doi:10.1021/ar0101584
- Li CH, Yao KF, Liang J (2003) Influence of acid treatments on the activity of carbon nanotube-supported catalysts. Carbon 41:858–860. doi:10.1016/S0008-6223(02)00450-5

26. Likholobov VA, Moroz BL (1997) In: Ertl G, Knozinger H, Weitkamp J (eds) Handbook of heterogeneous catalysis, vol 5. Wiley-VCH, Weinheim, p 2231
27. Sharghi H, Khalifeh R, Rashidi Z (2013) Synthesis of chromeno[3,4-b]quinoline derivatives by heterogeneous [Cu(II)BHPPDAH] catalyst without being immobilized on any support under mild conditions using PEG 300 as green solvent. *Mol Divers* 17:721–730. doi:10.1007/s11030-013-9468-4
28. Khalifeh R, Sharghi H, Rashidi Z (2013) Synthesis of [Zn(II)BHPPDAH] as new heterogeneous catalyst without being immobilized on any support and applied for mannich reaction. *Heteroatom Chem* 24:372–383. doi:10.1002/hc.21103
29. Sharghi H, Khoshnood A, Doroodmand MM, Khalifeh R (2012) 1,4-Dihydroxyanthraquinone-copper(II) nanoparticles immobilized on silica gel: a highly efficient, copper scavenger and recyclable heterogeneous nanocatalyst for a click approach to the three-component synthesis of 1,2,3-triazole derivatives in water. *J Iran Chem Soc* 9:231–250. doi:10.1007/s13738-011-0046-3
30. Sharghi H, Jokar M, Doroodmand MM, Khalifeh R (2010) Catalytic friedel-crafts acylation and benzylation of aromatic compounds using activated hematite as a novel heterogeneous catalyst. *Adv Synth Catal* 352:3031–3044. doi:10.1002/adsc.201000319
31. Sharghi H, Beyzavi MH, Safavi A, Doroodmand MM, Khalifeh R (2009) Immobilization of porphyrinatocopper nanoparticles onto activated multi-walled carbon nanotubes and a study of its catalytic activity as an efficient heterogeneous catalyst for a click approach to the three-component synthesis of 1,2,3-Triazoles in water. *Adv Synth Catal* 351:2391–2410. doi:10.1002/adsc.200900353
32. Sharghi H, Khalifeh R, Doroodmand MM (2009) Copper nanoparticles on charcoal for multicomponent catalytic synthesis of 1,2,3-triazole derivatives from benzyl halides or alkyl halides, terminal alkynes and sodium azide in water as a “Green” solvent. *Adv Synth Catal* 351:207–218. doi:10.1002/adsc.200800612
33. Savafi A, Maleki N, Doroodmand MM (2012) Comparative investigation of chemical vapor deposition of palladium nanoparticles on different carbon substrates. *Fuller Nanotubes Carbon Nanostruct* 20:56–71. doi:10.1080/1536383X.2010.533301
34. Olivero S, Dunach E (1997) Nickel-catalysed electroreductive cleavage of propargyl compounds. *Tetrahedron Lett* 38:6193–6196. doi:10.1016/S0040-4039(97)01396-8
35. Chakraborti AK, Sharma L, Nayak MK (2002) Demand-based thiolate anion generation under virtually neutral conditions: Influence of steric and electronic factors on chemo- and regioselective cleavage of aryl alkyl ethers. *J Org Chem* 67:6406–6414. doi:10.1021/jo0256540
36. Tanaka S, Saburi H, Ishibashi Y, Kitamura M (2004) CpRu^{II}PF₆/Quinaldic acid-catalyzed chemoselective allyl ether cleavage. A simple and practical method for hydroxyl deprotection. *Org Lett* 6:1873–1875. doi:10.1021/ol0493397
37. Bartoli G, Cupone G, Dalpozzo R, De Nino A, Maiuolo L, Marcantoni E, Procopio A (2001) Cerium-mediated deprotection of substituted allyl ethers. *Synlett* 12:1897–1900. doi:10.1055/s-2001-18746
38. Ishizaki M, Yamada M, Watanabe S, Hoshino O, Nishitani K, Hayashida M, Tanaka A, Hara H (2004) Palladium charcoal-catalyzed deprotection of *O*-allylphenols. *Tetrahedron* 60:7973–7981. doi:10.1016/j.tet.2004.05.097
39. Hwu JR, Wong FF, Huang J-J, Tsay S-C (1997) Sodium bis(trimethylsilyl)amide and lithium diisopropylamide in deprotection of alkyl aryl ethers: α -effect of silicon. *J Org Chem* 62:4097–4104. doi:10.1021/jo961191k
40. Ranu BC, Chattopadhyay K (2007) A new route to the synthesis of (E)- and (Z)-2-alkene-4-ynoates and Nitriles from vic-Diiodo-(E)-alkenes catalyzed by Pd(0) nanoparticles in water. *Org Lett* 9:2409–2412. doi:10.1021/ol0708121
41. Guibe F (1998) Allylic protecting groups and their use in a complex environment part II: allylic protecting groups and their removal through catalytic palladium π -allyl methodology. *Tetrahedron* 54:2967–3042. doi:10.1016/S0040-4020(97)10383-0